On the phenomenology of a two-Higgs-doublet model with maximal CP symmetry at the LHC

JHEP05(2009)028

(http://iopscience.iop.org/1126-6708/2009/05/028)

Published by IOP Publishing for SISSA

Received: *March 26, 2009*
Revised: *April 16, 2009*
Accepted: *April 23, 2009*
Published: *May 7, 2009*

On the phenomenology of a two-Higgs-doublet model with maximal CP symmetry at the LHC

M. Maniatis and O. Nachtmann

Institut für Theoretische Physik,
Philosophenweg 16, 69120 Heidelberg, Germany
E-mail: M.Maniatis@thphys.uni-heidelberg.de,
O.Nachtmann@thphys.uni-heidelberg.de

Abstract: Predictions for LHC physics are worked out for a two-Higgs-doublet model having four generalized CP symmetries. In this *maximally-CP-symmetric model* (MCPM) the first fermion family is, at tree level, uncoupled to the Higgs fields and thus massless. The second and third fermion families have a very symmetric coupling to the Higgs fields. But through the electroweak symmetry breaking a large mass hierarchy is generated between these fermion families. Thus, the fermion mass spectrum of the model presents a rough approximation to what is observed in Nature. In the MCPM there are, as in every two-Higgs-doublet model, five physical Higgs bosons, three neutral ones and a charged pair. In the MCPM the couplings of the Higgs bosons to the fermions are completely fixed. This allows us to present clear predictions for the production at the LHC and for the decays of the physical Higgs bosons. As salient feature we find rather large cross sections for Higgs boson production via Drell-Yan type processes. With experiments at the LHC it should be possible to check these predictions.

Keywords: Beyond Standard Model, Quark Masses and SM Parameters, Discrete and Finite Symmetries, Higgs Physics

ArXiv ePrint: 0901.4341

doi:10.1088/1126-6708/2009/05/028

JHEP05(2009)028

Contents

1 Introduction

The Standard Model (SM) of particle physics is very successful in describing the currently known experimental data; see [1] for a review. Nevertheless, the SM leaves open a number of theoretical questions. Thus, various extensions of the SM have been studied extensively. With the start-up of the LHC we can hope that experiments will soon give decisive answers in which way - if at all - the SM has to be extended; see [2] for a brief overview of these topics.

In this paper we shall study a particular two-Higgs-doublet model (THDM) and develop its LHC phenomenology. The model, which we want to call maximally-CP-symmetric model (MCPM) for reasons which will become clear later, has the field content as in the SM except for the Higgs sector, where we have two Higgs doublets instead of only one. Many versions of THDMs have been studied in the literature; see [3–16] and references therein. In our group we have studied various aspects of the most general THDM in [17, 18]. A class of interesting models having a maximal number of generalized CP symmetries was found. In [19] these models were studied in detail and it was shown that the requirement of maximal CP invariance led to a very interesting structure for the coupling of fermions to the Higgs fields. Maximal CP invariance requires more than one fermion family if fermions are to get non-zero masses. With the additional requirement of absence of flavor-changing neutral currents at tree level and of mass-degenerate massive fermions a unique Lagrangian was derived. This Lagrangian is very symmetric between the second and third

JHEP05(2009)028

fermion families *before* electroweak symmetry breaking (EWSB) occurs. But after EWSB the third family becomes massive, the second family stays massless. In this model also the first family is massless and the Cabibbo-Kobayashi-Maskawa (CKM) matrix equals the unit matrix. Of course, all this is not exactly as observed in Nature. But, on the other hand, it may be a starting point to understand some aspects of the large fermion mass hierarchies observed experimentally.

In the present paper we shall work out concrete predictions for LHC physics which follow from the two-Higgs-doublet model with maximal CP invariance, the MCPM, having the large fermion mass hierarchies as discussed in [19]. In section 2 we recall the main features of the Lagrangian. In section 3 we give our predictions for the decays of the physical Higgs particles of the MCPM. Section 4 deals with Higgs-boson production at the LHC. We draw our conclusions in section 5. In appendix A we give the explicit form of the Lagrangian and some Feynman rules of the MCPM. If the MCPM, in the strict symmetry limit, represents not too bad an approximation to the real world then this should also be true for its LHC phenomenology as discussed in this paper. Thus, our work should be considered as presenting the *generic features* of this phenomenology.

2 The model

A detailed study of the MCPM can be found in ref. [19]. Here we want to recall the motivation and the essential steps to construct this model.

The general gauge-invariant and renormalizable potential $V(\varphi_1, \varphi_2)$ of the two Higgs doublets φ_1 and φ_2 is a hermitian linear combination of the terms

$$\varphi_i^\dagger \varphi_j, \quad (\varphi_i^\dagger \varphi_j)(\varphi_k^\dagger \varphi_l)\,, \tag{2.1}$$

with $i, j, k, l \in \{1, 2\}$. The $\mathrm{SU}(2)_L \times \mathrm{U}(1)_Y$ invariant scalar products are arranged into the hermitian, positive semi definite, 2×2 matrix

$$\underline{K}(x) := \begin{pmatrix} \varphi_1^\dagger \varphi_1 & \varphi_2^\dagger \varphi_1 \\ \varphi_1^\dagger \varphi_2 & \varphi_2^\dagger \varphi_2 \end{pmatrix}. \tag{2.2}$$

Its decomposition reads

$$\underline{K}(x) = \frac{1}{2} \left(K_0(x) \mathbb{1}_2 + \mathbf{K}(x)\, \boldsymbol{\sigma} \right) \tag{2.3}$$

with Pauli matrices σ^a $(a = 1, 2, 3)$. In this way one defines the real *gauge-invariant functions*

$$\begin{aligned} K_0 &= \varphi_1^\dagger \varphi_1 + \varphi_2^\dagger \varphi_2, \quad & K_1 &= 2\,\mathrm{Re}\, \varphi_1^\dagger \varphi_2, \\ K_3 &= \varphi_1^\dagger \varphi_1 - \varphi_2^\dagger \varphi_2, \quad & K_2 &= 2\,\mathrm{Im}\, \varphi_1^\dagger \varphi_2\,. \end{aligned} \tag{2.4}$$

In terms of these functions the general THDM potential can be written in the simple form

$$\begin{aligned} V = {} & \xi_0\, K_0(x) + \boldsymbol{\xi}^\mathrm{T}\, \mathbf{K}(x) + \eta_{00}\, K_0^2(x) \\ & + 2\, K_0(x)\, \boldsymbol{\eta}^\mathrm{T}\, \mathbf{K}(x) + \mathbf{K}^\mathrm{T}(x)\, E\, \mathbf{K}(x)\,, \end{aligned} \tag{2.5}$$

with $\mathbf{K} = (K_1, K_2, K_3)^{\mathrm{T}}$ and parameters ξ_0, η_{00}, three-component vectors $\boldsymbol{\xi}$, $\boldsymbol{\eta}$ and the 3×3 matrix $E = E^{\mathrm{T}}$. All parameters in (2.5) are real.

One now proceeds to study CP transformations in the general THDM. Writing the Higgs potential in the form (2.5) one finds a simple geometric picture for CP transformations. The *standard* CP transformation ($\mathrm{CP_s}$) of the Higgs doublets is

$$\varphi_i(x) \xrightarrow{\mathrm{CP_s}} \varphi_i^*(x') , \qquad (i = 1, 2) , \tag{2.6}$$

where, due to the parity transformation $x' = (x_0, -\mathbf{x})^{\mathrm{T}}$. In terms of the gauge invariant functions, this $\mathrm{CP_s}$ transformation is simply $K_0(x) \to K_0(x')$ and

$$\begin{aligned} K_1(x) &\to K_1(x') , \\ K_2(x) &\to -K_2(x') , \\ K_3(x) &\to K_3(x') . \end{aligned} \tag{2.7}$$

Geometrically, this is a reflection on the 1–3 plane in $\mathbf{K}$ space in addition to the argument change. Motivated by this geometric picture, *generalized* CP transformations (CP_g) corresponding to reflections on planes ($\mathrm{CP}_g^{(ii)}$) as well as to the point reflection ($\mathrm{CP}_g^{(i)}$) in $\mathbf{K}$ space were studied in [18, 19]. The $\mathrm{CP}_g^{(i)}$ transformation is given by $K_0(x) \to K_0(x')$ and

$$\mathbf{K}(x) \to -\mathbf{K}(x') \tag{2.8}$$

and plays a central role in the construction of the MCPM. In [19] some distinguishing features of this transformation are discussed. In terms of the original Higgs doublets these CP_g transformations read generically

$$\varphi_i(x) \to W_{ij}\varphi_j^*(x') . \tag{2.9}$$

The 2×2 matrices W corresponding to the transformations $\mathrm{CP}_g^{(i)}$ and to $\mathrm{CP}_{g,a}^{(ii)}$ $(a = 1, 2, 3)$, the reflections on the coordinate planes in $\mathbf{K}$ space, are given in the second row of table 1, where we defined

$$\epsilon = \begin{pmatrix} 0 & 1 \\ -1 & 0 \end{pmatrix} . \tag{2.10}$$

The transformation $\mathrm{CP}_{g,2}^{(ii)}$ is, of course, just $\mathrm{CP_s}$ given in (2.6), (2.7). For $\mathrm{CP}_{g,1}^{(ii)}$ ($\mathrm{CP}_{g,3}^{(ii)}$) the transformation of the $\mathbf{K}$ vector is similar to (2.7) but with the sign change for K_1 (K_3).

Now we are in a position to recall the construction principles of the MCPM, that is, a THDM which respects all generalized CP symmetries of table 1. We start with the THDM Higgs potential (2.5). Requiring it to be symmetric under the generalized CP transformation $\mathrm{CP}_g^{(i)}$ leads with a suitable basis choice to

$$V(\varphi_1, \varphi_2) = \xi_0 K_0 + \eta_{00} K_0^2 + \mu_1 K_1^2 + \mu_2 K_2^2 + \mu_3 K_3^2 . \tag{2.11}$$

Note that here K_a, $(a = 1, 2, 3)$ enter only quadratically. This implies that the potential V of (2.11) is also invariant under the transformation $\mathrm{CP_s} \equiv \mathrm{CP}_{g,2}^{(ii)}$ which just changes the

JHEP05(2009)028

CP_g		W	U_R	U_L
point reflection	$\mathrm{CP}_g^{(i)}$	ϵ	ϵ	σ^1
2–3 plane reflection	$\mathrm{CP}_{g,1}^{(ii)}$	σ^3	$-\sigma^3$	$\mathbb{1}_2$
1–3 plane reflection	$\mathrm{CP}_{g,2}^{(ii)}$	$\mathbb{1}_2$	$\mathbb{1}_2$	$\mathbb{1}_2$
1–2 plane reflection	$\mathrm{CP}_{g,3}^{(ii)}$	σ^1	$-\sigma^1$	σ^1

Table 1. The matrices W of (2.9) and U_L and U_R of (2.12) for the four generalized CP invariances.

sign of the component K_2; see (2.7). Similarly one finds invariance of V (2.11) under $\mathrm{CP}_{g,1}^{(ii)}$ and $\mathrm{CP}_{g,3}^{(ii)}$. Thus, the potential is invariant under the point reflection symmetry (2.8) as well as all three different reflections on the coordinate planes in $\mathbf{K}$ space. In this way the Higgs potential of the MCPM is determined.

The next step is to extend these CP_g symmetries to the Yukawa terms, which couple the fermions $\psi(x)$ to the Higgs doublets. We define the generalized CP transformations of the fermions generically as

$$\begin{aligned}\mathrm{CP}_g\ :\quad &\psi_{\alpha\,L}(x) \to U_{L\,\alpha\beta}\,\gamma^0\,S(C)\,\bar{\psi}^{\mathrm{T}}_{\beta\,L}(x')\,,\\ &\psi_{\alpha\,R}(x) \to U_{R\,\alpha\beta}\,\gamma^0\,S(C)\,\bar{\psi}^{\mathrm{T}}_{\beta\,R}(x')\end{aligned} \tag{2.12}$$

with family indices α, β, $S(C) = i\gamma^2\gamma^0$ the usual matrix of charge conjugation, and unitary matrices U_L and U_R. As shown in the detailed study [19] having only one family coupled to the Higgs bosons in a $\mathrm{CP}_g^{(i)}$-symmetric way leads necessarily to vanishing Yukawa couplings, that is, to massless fermions. Thus, in the MCPM two families are coupled via Yukawa terms to the Higgs doublets. By convention these families are given the indices two and three. One finds that the Yukawa interactions are highly restricted requiring them to be invariant under the generalized CP transformations of table 1 for the fermions (2.12) and Higgs doublets (2.9). Moreover, the Yukawa couplings are uniquely defined, if in addition to these CP_g invariances one requires non-degenerate fermion masses and absence of large flavor-changing neutral currents (FCNCs). The corresponding matrices U_L and U_R are presented in the last two rows in table 1. Eventually, one ends up with the Yukawa part of the Lagrangian of the MCPM in the form

$$\begin{aligned}\mathscr{L}_{\mathrm{Yuk}}(x) = -c^{(1)}_{l\,3}\,\Bigg\{&\bar{\tau}_R(x)\,\varphi_1^\dagger(x)\begin{pmatrix}\nu_{\tau\,L}(x)\\ \tau_L(x)\end{pmatrix}\\ &-\bar{\mu}_R(x)\,\varphi_2^\dagger(x)\begin{pmatrix}\nu_{\mu\,L}(x)\\ \mu_L(x)\end{pmatrix}\Bigg\}\\ +c^{(1)}_{u\,3}\,\Bigg\{&\bar{t}_R(x)\,\varphi_1^{\mathrm{T}}(x)\,\epsilon\begin{pmatrix}t_L(x)\\ b_L(x)\end{pmatrix}\\ &-\bar{c}_R(x)\,\varphi_2^{\mathrm{T}}(x)\,\epsilon\begin{pmatrix}c_L(x)\\ s_L(x)\end{pmatrix}\Bigg\}\\ -c^{(1)}_{d\,3}\,\Bigg\{&\bar{b}_R(x)\,\varphi_1^\dagger(x)\begin{pmatrix}t_L(x)\\ b_L(x)\end{pmatrix}\end{aligned}$$

$$- \bar{s}_R(x)\, \varphi_2^\dagger(x) \begin{pmatrix} c_L(x) \\ s_L(x) \end{pmatrix} \Bigg\} + h.c. \tag{2.13}$$

where $c_{l\,3}^{(1)}$, $c_{u\,3}^{(1)}$ and $c_{d\,3}^{(1)}$ are real positive constants, determined by the fermion masses as discussed below. The first family remains uncoupled — at tree level — to the Higgs bosons in the MCPM.

Now we come to the questions of stability and EWSB in the MCPM. As discussed in [18, 19] the MCPM is stable, produces the correct breaking $\mathrm{SU}(2)_L \times \mathrm{U}(1)_Y \to \mathrm{U}(1)_{\mathrm{em}}$, and has no zero mass or mass degenerate Higgs bosons if and only if the parameters of V in (2.11) satisfy

$$\begin{aligned} \mu_1 > \mu_2 > \mu_3 \;&, \\ \eta_{00} > 0 \;&, \\ \mu_a + \eta_{00} > 0, \;& \qquad \text{for } a = 1,2,3 \;, \\ \xi_0 < 0 \;&, \\ \mu_3 < 0 \;&. \end{aligned} \tag{2.14}$$

Through EWSB only the Higgs doublet φ_1 gets a vacuum expectation value (VEV). In the unitary gauge we have

$$\varphi_1(x) = \frac{1}{\sqrt{2}} \begin{pmatrix} 0 \\ v_0 + \rho'(x) \end{pmatrix} \;, \tag{2.15}$$

$$\varphi_2(x) = \begin{pmatrix} H^+(x) \\ \frac{1}{\sqrt{2}}(h'(x) + ih''(x)) \end{pmatrix} \;, \tag{2.16}$$

where $\rho'(x)$, $h'(x)$ and $h''(x)$ are the real fields corresponding to the physical neutral Higgs particles. The fields $H^+(x)$ and $H^-(x) = \big(H^+(x)\big)^*$ correspond to the physical charged Higgs pair. In (2.15) v_0 is the standard VEV

$$v_0 \approx 246 \text{ GeV} \;, \tag{2.17}$$

which is given in terms of the original potential parameters of (2.11) by

$$v_0 = \sqrt{\frac{-\xi_0}{\eta_{00} + \mu_3}} \;. \tag{2.18}$$

Inserting (2.15) and (2.16) into (2.4) and (2.11) it is straightforward to calculate the masses of the physical Higgs fields in terms of the original parameters

$$\begin{aligned} m_{\rho'}^2 &= 2(-\xi_0) \;, \\ m_{h'}^2 &= 2v_0^2(\mu_1 - \mu_3) \;, \\ m_{h''}^2 &= 2v_0^2(\mu_2 - \mu_3) \;, \\ m_{H^\pm}^2 &= 2v_0^2(-\mu_3) \;. \end{aligned} \tag{2.19}$$

Conversely, one can express the original parameters $\xi_0, \dots, \mu_3$ by v_0 and the Higgs-boson masses

$$\begin{aligned}
\xi_0 &= -\frac{1}{2} m_{\rho'}^2 \,, \\
\eta_{00} &= \frac{1}{2v_0^2}(m_{H^\pm}^2 + m_{\rho'}^2) \,, \\
\mu_1 &= \frac{1}{2v_0^2}(m_{h'}^2 - m_{H^\pm}^2) \,, \\
\mu_2 &= \frac{1}{2v_0^2}(m_{h''}^2 - m_{H^\pm}^2) \,, \\
\mu_3 &= -\frac{1}{2v_0^2} m_{H^\pm}^2 \,.
\end{aligned} \tag{2.20}$$

The stability and correct $\mathrm{SU}(2)_L \times \mathrm{U}(1)_Y$ symmetry breaking conditions (2.14) require positive squared masses and

$$m_{h'}^2 > m_{h''}^2 \,. \tag{2.21}$$

Thus, (2.21) is the only strict relation for the Higgs-boson masses which one gets in the MCPM. On the other hand, if we require that the Higgs sector has weak couplings only, we should have η_{00}, $|\mu_1|$, $|\mu_2|$ and $|\mu_3|$ to be less than or equal to a number of $\mathcal{O}(1)$. From (2.19) we expect then that the masses of h', h'' and $H^\pm$ should be less than about $2v_0 \approx 500\,\mathrm{GeV}$. But by no means should this be considered as a necessary upper bound for the Higgs-boson masses in the MCPM.

Upon EWSB the Yukawa term (2.13) produces masses for the charged fermions of the third family. Inserting (2.15) and (2.16) into (2.13) gives

$$\begin{aligned}
m_\tau &= c_{l\,3}^{(1)} \frac{v_0}{\sqrt{2}} \,, \\
m_t &= c_{u\,3}^{(1)} \frac{v_0}{\sqrt{2}} \,, \\
m_b &= c_{d\,3}^{(1)} \frac{v_0}{\sqrt{2}} \,.
\end{aligned} \tag{2.22}$$

The fermions of the second and the first families stay massless in the fully-symmetric theory at tree level. Of course, this is only an approximation valid for the tree-level investigations. Fortunately, from the numerical studies which follow below, we will see that the main features of the LHC phenomenology of the MCPM are insensitive to the first- and second-family masses due to their smallness.

The next task is to express the Lagrangian of the MCPM in terms of the physical fields in the unitary gauge. This is done in appendix A. From there the Feynman rules of the MCPM can be read off. In appendix A we give these rules for the three-point vertices which are relevant for us in the following. Some salient features are as follows.

- The neutral Higgs boson ρ' couples to the third-family fermions as the physical Higgs boson ρ'_{SM} of the SM.

- The neutral Higgs boson h' has a scalar coupling to the *second*-family fermions. The Higgs boson h'' which is lighter than h' has a pseudoscalar coupling to the *second*-family fermions. But the coupling constants for h' and h'' are proportional to the masses of the *third*-family fermions, that is, to m_τ, m_t and m_b.

- Also the charged Higgs bosons $H^\pm$ couple only to the second-family fermions but again with coupling constants proportional to the masses of the third-family fermions.

As we shall see in the following these features lead to quite distinct phenomenological predictions of the MCPM for LHC physics.

We summarize this section. We have recalled the construction principles of the model which has the four generalized CP symmetries of table 1. As can easily be seen from (2.11) this is the maximal number of such symmetries, including $\mathrm{CP}_g^{(i)}$, one can have in a THDM if one requires absence of zero mass and mass degenerate physical Higgs bosons. Thus, the name *maximally-CP-symmetric model*, MCPM, seems justified. The extension of the four generalized CP symmetries to the Yukawa interaction gave drastic restrictions for the family structure of the model and led, finally, with some additional arguments to the coupling (2.13). The remaining sections of this paper are devoted to discussing physical consequences of the MCPM.

3 Higgs-boson decays

The decays of the Higgs particles of the MCPM which are possible at tree level can be directly read off from the Lagrangian in the form given in (A.5) of appendix A. We have decays of a Higgs particle into a fermion and an antifermion, and of a Higgs particle into another Higgs particle plus a gauge boson W or Z. Furthermore, we could have decays of one Higgs boson into two other Higgs bosons and one Higgs boson into another Higgs boson plus two gauge bosons if the mass differences of the various Higgs bosons are large enough. In the following we shall restrict ourselves to discussing the tree-level results for the fermionic and the Higgs boson plus gauge boson decays and the results for the loop-induced two-photon and two-gluon decays.

3.1 Fermionic decays

The generic fermionic decay of a Higgs particle H_1 is

$$H_1(k) \to f'(p_1) + \bar{f}(p_2) \tag{3.1}$$

where f and f' denote the fermions and the momenta are indicated in brackets. The corresponding diagram and analytic expression at tree level for the vertex are shown in figure 1. The possible decays together with the corresponding coupling constants a and b are listed in table 2. There, N_c^f is the color factor which equals 1 for leptons and 3 for

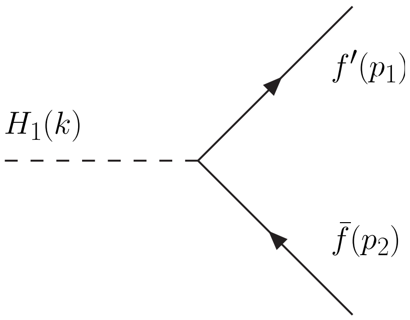

$$-i\frac{1}{v_0}(a + b\,\gamma_5)$$

Figure 1. The diagram for the generic decay $H_1 \to f'\bar{f}$ and the corresponding analytic expression for the vertex.

H_1	f'	$\bar{f}$	a	b	$\lvert a\rvert^2 + \lvert b\rvert^2$	N_c^f
ρ'	τ	$\bar{\tau}$	m_τ	0	m_τ^2	1
	t	$\bar{t}$	m_t	0	m_t^2	3
	b	$\bar{b}$	m_b	0	m_b^2	3
h'	μ	$\bar{\mu}$	$-m_\tau$	0	m_τ^2	1
	c	$\bar{c}$	$-m_t$	0	m_t^2	3
	s	$\bar{s}$	$-m_b$	0	m_b^2	3
h''	μ	$\bar{\mu}$	0	$-im_\tau$	m_τ^2	1
	c	$\bar{c}$	0	im_t	m_t^2	3
	s	$\bar{s}$	0	$-im_b$	m_b^2	3
H^+	ν_μ	$\bar{\mu}$	$-m_\tau/\sqrt{2}$	$-m_\tau/\sqrt{2}$	m_τ^2	1
	c	$\bar{s}$	$(m_t - m_b)/\sqrt{2}$	$-(m_t + m_b)/\sqrt{2}$	$m_t^2 + m_b^2$	3
H^-	μ	$\bar{\nu}_\mu$	$-m_\tau/\sqrt{2}$	$m_\tau/\sqrt{2}$	m_τ^2	1
	s	$\bar{c}$	$(m_t - m_b)/\sqrt{2}$	$(m_t + m_b)/\sqrt{2}$	$m_t^2 + m_b^2$	3

Table 2. The fermionic decays of the Higgs particles in the MCPM and the corresponding coupling constants a and b of figure 1.

quarks. The decay rate for the generic decay (3.1) is calculated as

$$\Gamma(H_1 \to f' + \bar{f}) = \frac{N_c^f}{8\pi v_0^2}\frac{w(m_{H_1}^2, m_f^2, m_{f'}^2)}{m_{H_1}^2}\, m_{H_1}\, \theta(m_{H_1} - m_f - m_{f'})$$
$$\times\left\{\lvert a\rvert^2 + \lvert b\rvert^2 - \frac{(m_f + m_{f'})^2}{m_{H_1}^2}\lvert a\rvert^2 - \frac{(m_f - m_{f'})^2}{m_{H_1}^2}\lvert b\rvert^2\right\}. \quad (3.2)$$

Here θ is the step function and

$$w(x, y, z) = \left(x^2 + y^2 + z^2 - 2xy - 2yz - 2zx\right)^{1/2} \quad (3.3)$$

is the usual kinematic function. Inserting in (3.2) the values a and b from table 2 we get the results for the individual decay rates as discussed below. For the fermion masses we use the values from [1].

The rates for the decays of ρ' to $t\bar{t}$ and $b\bar{b}$ are, at tree level, as for the SM Higgs particle ρ'_{SM}. In the strict symmetry limit of the MCPM, as we discuss it here, the first-

decay	partial width Γ [GeV]
$h' \to c\bar{c}$	12.08 $(m_{h'}/200\ \text{GeV})$
$h'' \to c\bar{c}$	12.08 $(m_{h''}/200\ \text{GeV})$
$H^+ \to c\bar{s}$	12.09 $(m_{H^\pm}/200\ \text{GeV})$
$H^- \to s\bar{c}$	12.09 $(m_{H^\pm}/200\ \text{GeV})$

Table 3. The partial widths for the leading fermionic decays of h', h'', H^+ and H^-. The Higgs-boson masses have to be inserted in units of GeV.

and second-family fermions are massless and ρ' will not decay to them at tree level. In reality this will, of course, be only an approximation. In Nature we find very small but non-zero values for the ratios of first- and second-family masses to the corresponding third family masses; see (125) of [19]. Thus, we should conclude that the Higgs particle ρ' of the MCPM has the decays to second- and first-family fermions highly suppressed as is also the case for the SM Higgs boson ρ'_{SM}.

For the Higgs particles h', h'', H^+ and H^- the dominant fermionic decays are according to table 2

$$\begin{aligned} h' &\to c\bar{c}\,, \\ h'' &\to c\bar{c}\,, \\ H^+ &\to c\bar{s}\,, \\ H^- &\to s\bar{c}\,. \end{aligned} \tag{3.4}$$

The numerical results for the decay widths with the s and c quark masses set to zero are given in table 3. Note that these partial decay widths are proportional to the respective Higgs-boson mass.

3.2 Decays of a Higgs particle into another Higgs particle plus a gauge boson

Here we discuss the decays

$$H_1(k) \to H_2(p_1) + V(p_2)\ , \tag{3.5}$$

where H_1 and H_2 generically denote Higgs particles and V a gauge boson, $V = Z, W^\pm, \gamma$. In (3.5) the momenta are indicated in brackets. The decay (3.5) can, of course, only proceed if $m_{H_1} \geq m_{H_2} + m_V$. The generic tree level diagram and the analytic expression for the vertex for the decay (3.5) are shown in figure 2. In the MCPM h' always has higher mass than h''; see (2.21). Also, no decays (3.5) with $V = \gamma$ occur at tree level. This leaves us with the decays shown in table 4, where we also list the corresponding values for the coupling constant C in the vertex diagram in figure 2. The decay rate for the process (3.5) is easily calculated:

$$\begin{aligned} \Gamma(H_1 \to H_2 + V) = {} & \frac{\alpha}{4}|C|^2\, \theta(m_{H_1} - m_{H_2} - m_V)\, m_{H_1} \left(\frac{m_{H_1}}{m_V}\right)^2 \\ & \times \left(1 - \frac{(m_{H_2} + m_V)^2}{m_{H_1}^2}\right)^{3/2} \left(1 - \frac{(m_{H_2} - m_V)^2}{m_{H_1}^2}\right)^{3/2} . \end{aligned} \tag{3.6}$$

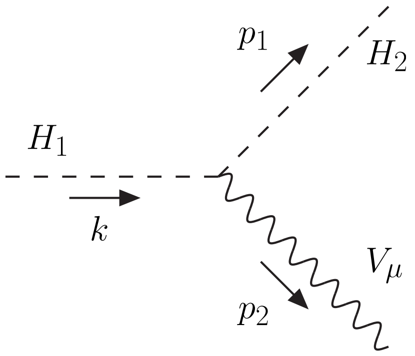

$$ie\, C\, (k + p_1)_\mu$$

Figure 2. The generic tree level diagram and vertex expression for the decay (3.5)

H_1	H_2	V	C
h'	h''	Z	$-i/(2s_W c_W)$
h'	H^+	W^-	$-1/(2s_W)$
h'	H^-	W^+	$1/(2s_W)$
h''	H^+	W^-	$-i/(2s_W)$
h''	H^-	W^+	$-i/(2s_W)$
H^+	h'	W^+	$-1/(2s_W)$
H^+	h''	W^+	$i/(2s_W)$
H^-	h'	W^-	$1/(2s_W)$
H^-	h''	W^-	$i/(2s_W)$

Table 4. The decays (3.5) occurring at tree level in the MCPM if the masses satisfy $m_{H_1} > m_{H_2} + m_V$. The last column gives the corresponding coupling constant C in figure 2. Here $s_W \equiv \sin\theta_W$ and $c_W \equiv \cos\theta_W$ denote the sine and the cosine of the weak mixing angle, respectively

Here $\alpha = e^2/(4\pi)$ is the fine structure constant. The coupling constants C in (3.6) are given in table 4.

The partial width for the decay of the h' boson into the h'' boson and an additional Z-boson is shown as function of the h' mass for fixed h'' masses in figure 3. We see that we get a width exceeding 10 GeV only for rather large mass differences of the two involved Higgs bosons. Considering for instance $m_{h''} = 100\,\text{GeV}$ we get from figure 3 $\Gamma > 10\,\text{GeV}$ only for $m_{h'} > 364\,\text{GeV}$. For $m_{h''} = 300\,\text{GeV}$, $\Gamma > 10\,\text{GeV}$ is reached only for $m_{h'} > 517\,\text{GeV}$. For the charged Higgs boson decays into a neutral Higgs boson and a W boson we get quite similar results.

3.3 Decays of neutral Higgs bosons into a photon pair

Here we discuss the decays

$$H_1(k) \to \gamma(p_1) + \gamma(p_2) \tag{3.7}$$

in the MCPM where H_1 generically denotes a neutral Higgs particle,

$$H_1 = \rho', h', h'' . \tag{3.8}$$

JHEP05(2009)028

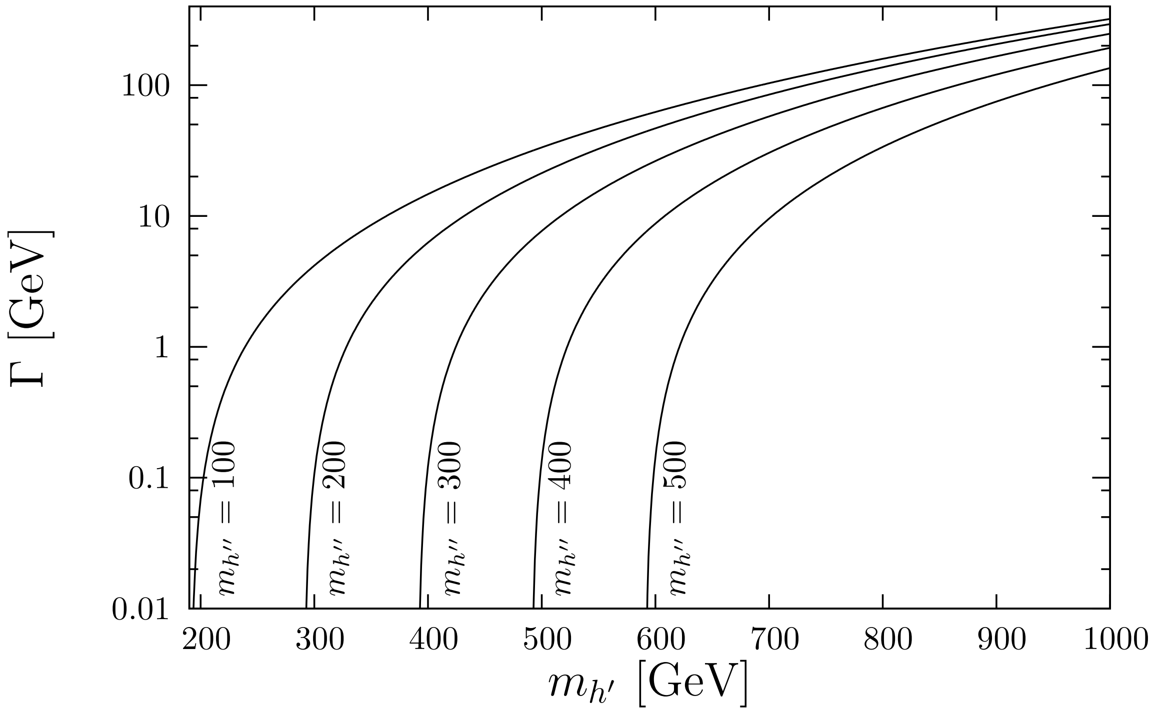

Figure 3. Partial width of the decay $h' \to h'' + Z$. Shown is this width as function of the Higgs-boson mass $m_{h'}$ for different fixed masses $m_{h''}$ from 100 to 500 GeV in steps of 100 GeV.

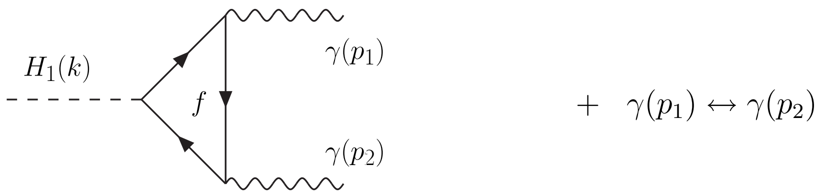

Figure 4. Leading order diagrams for the decay $H_1 \to \gamma\gamma$ (3.7) with a loop of a fermion f.

We have to consider in general contributions to the decay (3.7) via a fermion loop, a W-boson loop and a loop of a charged Higgs boson. In figure 4 the Feynman diagram for the contribution of a fermion loop is shown.

The couplings of the Higgs bosons (3.8) to the fermions, the W-boson and the charged Higgs bosons are given in the Feynman rules in appendix A.

For the calculation of the decay rate for (3.7) we rely on the results of [4] which give

$$\Gamma(H_1 \to \gamma + \gamma) = \frac{\alpha^2}{256\pi^3} \frac{m_{H_1}^3}{v_0^2} \left| \sum_{i=f,W,H^\pm} I_{H_1}^i \right|^2 . \tag{3.9}$$

The contributions of the various loops are as follows:

- fermion loops,

$$I_{H_1}^f = 4N_c^f\ e_f^2\ R_f^{H_1}/m_{H_1}^2\ F_{\frac{1}{2}}^{H_1}\left(\frac{4m_f^2}{m_{H_1}^2}\right) \tag{3.10}$$

with e_f the charge of the fermion in units of the positron charge, N_c^f the color factor and

$$R_f^{H_1} = \begin{cases} m_f^2, & \text{for } H_1 = \rho', f = t, b, \tau \\ -m_t m_c, & \text{for } H_1 = h', f = c \\ -m_b m_s, & \text{for } H_1 = h', f = s \\ -m_\tau m_\mu, & \text{for } H_1 = h', f = \mu \\ -m_t m_c, & \text{for } H_1 = h'', f = c \\ m_b m_s, & \text{for } H_1 = h'', f = s \\ m_\tau m_\mu, & \text{for } H_1 = h'', f = \mu \\ 0, & \text{otherwise} \ . \end{cases} \tag{3.11}$$

Furthermore we set

$$F_{\frac{1}{2}}^{H_1}(z) = \begin{cases} -2\big[1 + (1-z)f(z)\big], & \text{for } H_1 = \rho', h' \\ -2f(z), & \text{for } H_1 = h'' \ . \end{cases} \tag{3.12}$$

- W-boson loop,

$$I_{h'}^W = 0, \quad I_{h''}^W = 0, \quad I_{\rho'}^W = F_1\left(\frac{4m_W^2}{m_{\rho'}^2}\right) \tag{3.13}$$

with

$$F_1(z) = 2 + 3z + 3z(2-z)f(z) \ . \tag{3.14}$$

- $H^\pm$-boson loop,

$$I_{h'}^{H^\pm} = 0, \quad I_{h''}^{H^\pm} = 0, \quad I_{\rho'}^{H^\pm} = \frac{m_{\rho'}^2 + 2m_{H^\pm}^2}{2m_{H^\pm}^2} F_0\left(\frac{4m_{H^\pm}^2}{m_{\rho'}^2}\right) \tag{3.15}$$

with

$$F_0(z) = z\big[1 - zf(z)\big] \ . \tag{3.16}$$

Finally, $f(z)$ is defined as

$$f(z) = \begin{cases} -\frac{1}{4}\left[\ln\left(\frac{1+\sqrt{1-z}}{1-\sqrt{1-z}}\right) - i\pi\right]^2, & \text{for } 0 < z < 1 \\ \big[\arcsin(\sqrt{1/z})\big]^2, & \text{for } z \geq 1 \ . \end{cases} \tag{3.17}$$

For the decays of the neutral Higgs bosons into a photon pair we find only small widths from these results. The partial decay width of the ρ' boson is compared to the corresponding width of the ρ'_{SM} in figure 5. We get significant deviations of the 2γ decay widths of the ρ' boson and the SM boson ρ'_{SM} only if $m_{\rho'}$ is near to or higher than twice the charged Higgs-boson mass which we set to $m_{H^\pm} = 250\,\mathrm{GeV}$ in this plot. Of course, the peak at twice the charged Higgs-boson mass is an artifact due to our neglect of the finite width of $H^\pm$ in the calculation. The peak will become a broader structure if the non-vanishing $H^\pm$ width is taken into account. Let us note that even for large charged Higgs-boson masses the corresponding loop contribution does not decouple. This comes about as follows. Consider the diagram of figure 4 with a $H^\pm$ loop instead of the fermion loop f. The $\rho' H^+ H^-$ coupling contains a factor $m^2_{H^\pm}$; see (A.5) in appendix A. The loop integration gives for large $m^2_{H^\pm}$, using simple power counting arguments, a factor $1/m^2_{H^\pm}$. The net result is a finite contribution to the amplitude $\rho' \to \gamma\gamma$ even for large $m^2_{H^\pm}$. This is, of course, borne out by the explicit calculation in (3.15) from which we find

$$I^{H^\pm}_{\rho'} \to -\frac{1}{3} \tag{3.18}$$

for $m_{H^\pm} \to \infty$ keeping $m_{\rho'}$ fixed.

For masses of the $\rho'_{\rm SM}$ boson of 120 to 150 GeV the decay channel $\rho'_{\rm SM} \to \gamma\gamma$ is an important discovery mode at the LHC. We find here that the 2γ width of $\rho'_{\rm SM}$ and of the ρ' in the MCPM are quite similar for this mass range if $m_{H^\pm} > 200$ GeV. As we shall show below in section 4.2 also the production cross sections for ρ' and $\rho'_{\rm SM}$ are practically equal. Thus, in the above mass range, the 2γ channel is as good a discovery channel for ρ' as it is for $\rho'_{\rm SM}$.

We turn now to the 2γ decays of h' and h''. We see from (3.10), (3.13) and (3.15) that here only the fermion loops contribute. This comes about since there are no couplings linear in h' or h'' to a W^+W^- and a H^+H^- pair in the MCPM; see (A.5) of appendix A. The only fermion flavors which contribute at one loop level to the 2γ decays of h' and h'' are the c and s quarks and the muon μ. In the strict symmetry limit of the MCPM these fermions are massless. Of course, in reality they get masses. Thus we have kept these masses in the loop calculation. The structure of the results can be seen from (3.9)–(3.12). Let us consider as an example the c-quark-loop contribution to $h' \to \gamma\gamma$. The factor $I^c_{h'}$ (3.10) contains $R^{h'}_c = -m_t m_c$ where m_t originates from the $h' c\bar{c}$ vertex (see the Feynman rules in the appendix), whereas m_c comes from the loop integration. The term $F^{h'}_{\frac{1}{2}}(4m_c^2/m_{h'}^2)$ is proportional to $\ln^2(m_{h'}/m_c)$ for $m_c \to 0$. Thus, $I^c_{h'}$ vanishes for $m_c \to 0$. For the muon and s-quark loops the discussion is analogous. In the strict symmetry limit of the MCPM where $m_c = m_s = m_\mu = 0$ we have, therefore, $\Gamma(h' \to \gamma\gamma) = \Gamma(h'' \to \gamma\gamma) = 0$. In order to get a reasonable estimate for these rates we keep the finite fermion masses in the loop calculation. This estimate gives tiny partial rates. For the h' and h'' decays into a photon pair we find partial widths rising to about 3.5 keV for Higgs-boson masses increasing from zero up to 35 GeV. For Higgs-boson masses higher than 35 GeV the partial widths decrease monotonically with increasing masses. Thus, these partial widths are never larger than 3.5 keV which is very small compared to the decay widths of the main fermionic modes of table 3.

3.4 Decays of neutral Higgs bosons into two gluons

Here we discuss the decays

$$H_1(k) \to G(p_1) + G(p_2) \tag{3.19}$$

JHEP05(2009)028

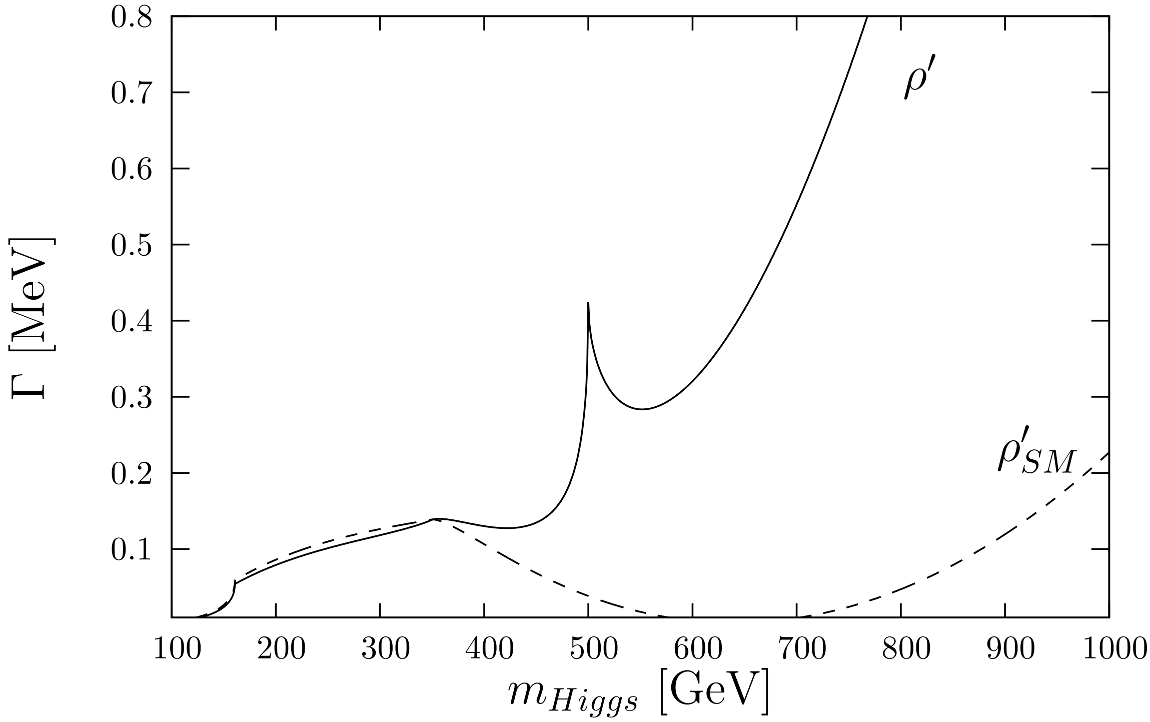

Figure 5. Partial decay widths of the neutral Higgs boson ρ' and of the SM Higgs boson ρ'_{SM} into a pair of photons. The charged Higgs-boson mass is supposed to be $m_{H^\pm} = 250\,\text{GeV}$.

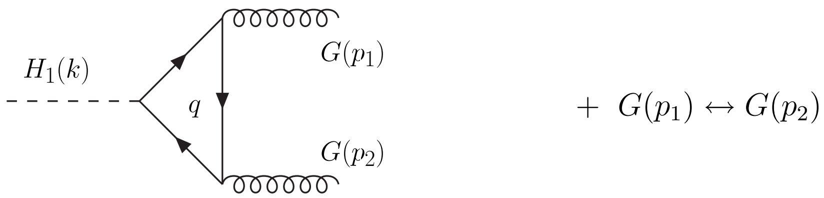

Figure 6. Leading order diagrams for the decay $H_1 \to GG$ (3.19) with one loop of a quark q.

in the MCPM where H_1 generically denotes a neutral Higgs particle (3.8). The leading contributions to the decay (3.19) proceed via quark loops as shown in figure 6.

The calculation of the diagrams of figure 6 is quite analogous to that for the two-photon decay with an internal quark loop; see figure 4. Of course, in the gluon pair decay there are no contributions of a W-boson and a $H^\pm$ in the loop. Replacing α by the strong coupling parameter α_s and changing the color factor appropriately we get

$$\Gamma(H_1 \to G + G) = \frac{\alpha_s^2}{128\pi^3} \frac{m_{H_1}^3}{v_0^2} \left| \sum_{q=c,s,t,b} \tilde{I}_{H_1}^q \right|^2 \tag{3.20}$$

with

$$\tilde{I}_{H_1}^q = (4R_q^{H_1}/m_{H_1}^2)\, F_{\frac{1}{2}}^{H_1}(4m_q^2/m_{H_1}^2) \tag{3.21}$$

and the factors $R_q^{H_1}$ from (3.11) for the different contributions of the quark flavors and the function $F_{\frac{1}{2}}^{H_1}$ from (3.12). Explicitly (3.20) reads for the neutral Higgs bosons ρ', h' and h'':

$$\Gamma(\rho' \to G+G) = \frac{\alpha_s^2}{128\pi^3}\frac{m_{\rho'}^3}{v_0^2}\left|4\frac{m_t^2}{m_{\rho'}^2}F_{\frac{1}{2}}^{\rho'}\left(\frac{4m_t^2}{m_{\rho'}^2}\right)+4\frac{m_b^2}{m_{\rho'}^2}F_{\frac{1}{2}}^{\rho'}\left(\frac{4m_b^2}{m_{\rho'}^2}\right)\right|^2 , \tag{3.22}$$

$$\Gamma(h' \to G+G) = \frac{\alpha_s^2}{128\pi^3}\frac{m_{h'}^3}{v_0^2}\left|4\frac{m_t m_c}{m_{h'}^2}F_{\frac{1}{2}}^{h'}\left(\frac{4m_c^2}{m_{h'}^2}\right)+4\frac{m_b m_s}{m_{h'}^2}F_{\frac{1}{2}}^{h'}\left(\frac{4m_s^2}{m_{h'}^2}\right)\right|^2 \tag{3.23}$$

and

$$\Gamma(h'' \to G+G) = \frac{\alpha_s^2}{128\pi^3}\frac{m_{h''}^3}{v_0^2}\left|4\frac{m_t m_c}{m_{h''}^2}F_{\frac{1}{2}}^{h''}\left(\frac{4m_c^2}{m_{h''}^2}\right)-4\frac{m_b m_s}{m_{h''}^2}F_{\frac{1}{2}}^{h''}\left(\frac{4m_s^2}{m_{h''}^2}\right)\right|^2 . \tag{3.24}$$

For the numerics we take the strong coupling at the Z-mass scale, $\alpha_s = 0.12$ and $m_t = 171\,\text{GeV}$.

Now we discuss the result (3.20)–(3.24). Let us first consider the decay rate for $\rho' \to G+G$. The one-loop contributions from the t and b quarks are identical to the corresponding SM expressions. In the strict symmetry limit of the MCPM the other quarks, c, s, u and d are massless and do not contribute to $\rho' \to GG$ at one loop level. In reality we thus expect that their contribution is very small. The same is true in the SM where the c, s, u and d quarks together give only a 0.005% contribution to the decay width for $\rho'_{\text{SM}} \to GG$. Thus we find that in the MCPM the decay rate for $\rho' \to GG$ is practically as in the SM for ρ'_{SM}.

Turning now to the decays $h' \to GG$ and $h'' \to GG$ we must clearly say that in the strict symmetry limit of the MCPM where $m_c = m_s = 0$ we have $\Gamma(h' \to GG) = \Gamma(h'' \to GG) = 0$; see (3.23) and (3.24). But we can argue that in reality m_c and m_s are unequal to zero. Then, the Higgs particles h' and h'' with the couplings to c and s quarks given in appendix A will indeed decay into two gluons. The dominant contributions come from the c quark loops since the couplings of h' and h'' to c quarks are proportional to the large t-quark mass. But even with this enhancement factor we find only partial widths of the order of MeV for the decays $h' \to GG$ and $h'' \to GG$, respectively; see figure 7. Comparing with the results for the dominant fermionic decay modes of h' and h'' as shown in table 3 we find that the branching ratios for $h' \to GG$ and $h'' \to GG$ are predicted to be less than about 10^{-4}. Nevertheless, the results for the gluonic decays (3.19) will be needed for the discussion of the Higgs-boson production processes in the following section.

We summarize our findings for the Higgs-boson decays.

Firstly, we have results valid in the strict symmetry limit. We find that the ρ' decays are in essence as for the SM Higgs boson ρ'_{SM}. Only if $m_{\rho'}$ comes near to or is larger than $2m_{H^\pm}$ we do find large deviations between $\Gamma(\rho' \to \gamma\gamma)$ and $\Gamma(\rho'_{\text{SM}} \to \gamma\gamma)$. If the Higgs particles h', h'' and $H^\pm$ have masses below about 400 GeV their main decays are the fermionic ones as given in (3.4) and table 3. These rates can be taken as good estimates for the total decay rates of h', h'' and $H^\pm$, respectively. From (3.2) and table 2 we can

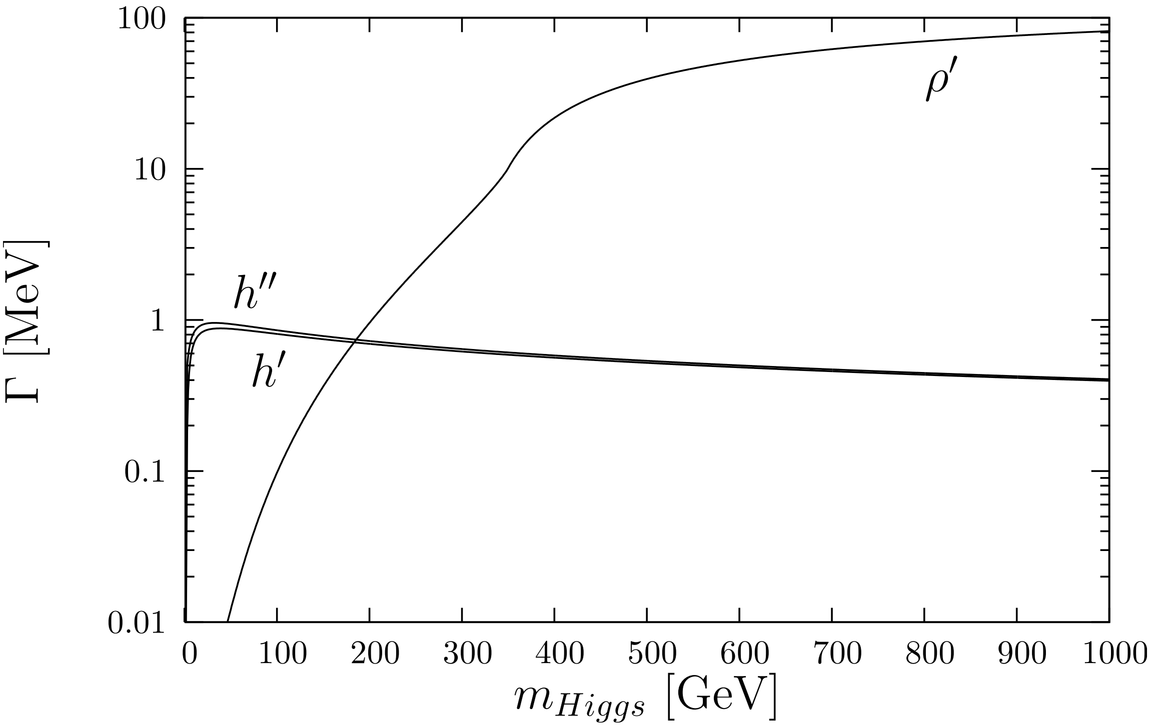

Figure 7. Partial decay widths of the neutral Higgs bosons into a pair of gluons.

estimate the branching ratios for the decays into leptons of the second family as

$$\begin{aligned}
&\frac{\Gamma(h' \to \mu^- \mu^+)}{\Gamma(h' \to \text{all})} \approx \frac{\Gamma(h'' \to \mu^- \mu^+)}{\Gamma(h'' \to \text{all})} \approx \\
&\frac{\Gamma(H^+ \to \mu^+ \nu_\mu)}{\Gamma(H^+ \to \text{all})} \approx \frac{\Gamma(H^- \to \mu^- \bar{\nu}_\mu)}{\Gamma(H^- \to \text{all})} \approx \\
&\frac{m_\tau^2}{3(m_t^2 + m_b^2) + m_\tau^2} \approx 3 \times 10^{-5}\,.
\end{aligned} \tag{3.25}$$

In the symmetry limit the Higgs particles h', h'' and $H^\pm$ do not couple to the fermions of the first and third families. Thus, the branching ratios for the decays of the Higgs-bosons h', h'' and $H^\pm$ to leptons of the first and third families are predicted to be very small in the MCPM. Note that this predicted large suppression of the decay modes involving τ and ν_τ leptons relative to the modes involving μ and ν_μ is a feature of the MCPM which distinguishes it from more conventional THDMs.

Secondly, we have estimates going beyond the strict symmetry limit, where the masses of the second- and first-family fermions are zero. In the strict limit the decay rates $\Gamma(h' \to \gamma\gamma) = \Gamma(h'' \to \gamma\gamma) = \Gamma(h' \to GG) = \Gamma(h'' \to GG) = 0$. Of course, in reality these decay rates will be non-zero. We have given *estimates* for these decay rates using the physical values for the masses of the second- and first-family fermions in the corresponding loop calculations. These estimates give very small values for the above decay rates which, therefore, do not change the overall picture significantly. As an example we show in figure 8 the branching ratios for the h'' Higgs-boson decays for the channels $c\bar{c}$, $s\bar{s}$, $\mu\bar{\mu}$, $H^\pm W^\mp$,

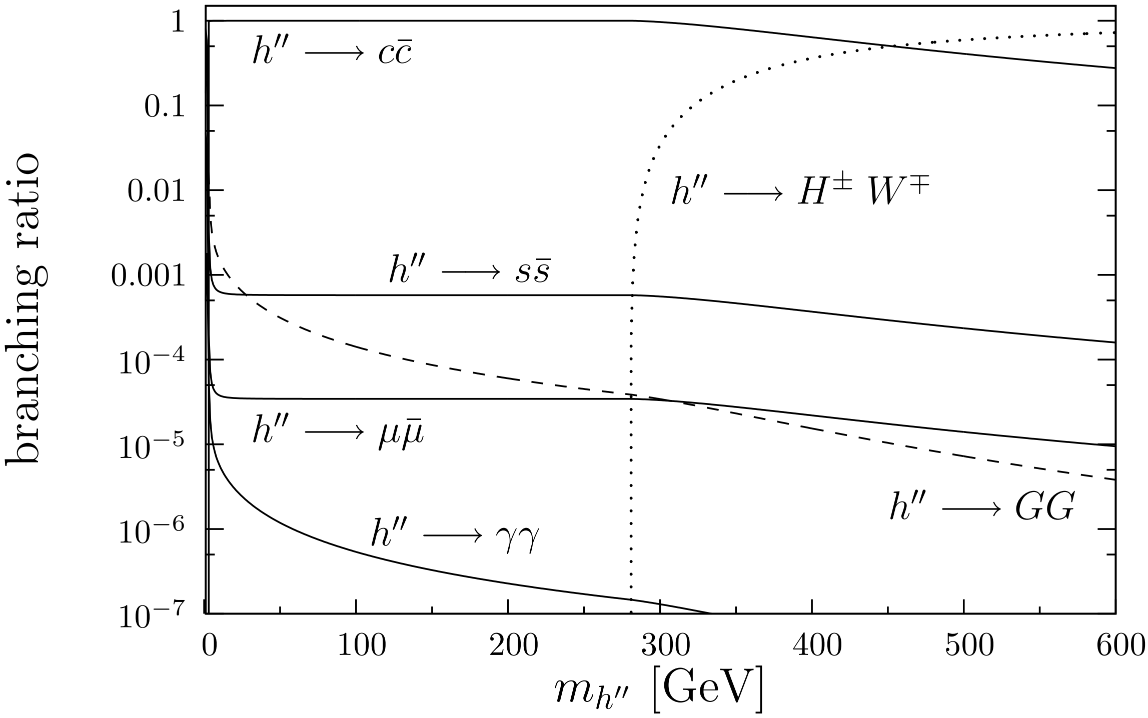

Figure 8. Branching fractions for the h'' Higgs-boson decays into different available decay channels as functions of $m_{h''}$. It is supposed that $m_{H^\pm} = 200\,\text{GeV}$. The curve for $h'' \to H^\pm W^\mp$ corresponds to the sum of these two channels.

GG and $\gamma\gamma$. It is supposed that the charged Higgs bosons $H^\pm$ have a mass of 200 GeV. As another example we show in figure 9 the branching ratios for the decays of the H^+ boson as function of its mass m_{H^+} supposing $m_{h'} = 250\,\text{GeV}$ and $m_{h''} = 180\,\text{GeV}$.

4 Higgs-boson production

In this section we shall discuss the production of Higgs particles in proton-proton collisions at LHC energies. We write generically

$$p(p_1) + p(p_2) \to H_1(k) + X \; , \tag{4.1}$$

where H_1 denotes one of the Higgs particles of the MCPM; $H_1 = \rho', h', h'', H^\pm$. There are, of course, many contributions to (4.1). For a discussion of the contributions to ρ'_{SM} production in the framework of the SM see for instance [20].

We shall focus here on two different Higgs-boson production mechanisms in the MCPM, the quark-antiquark fusion and the gluon-gluon fusion. As we shall see, we get in both cases results which are quite distinct from those obtained in more conventional THDMs; see for instance [21].

4.1 Higgs-boson production by quark-antiquark fusion

Here we investigate the contribution to (4.1) from the quark-antiquark fusion, that is, the Drell-Yan type process. The generic diagram is shown in figure 10. The fusion processes

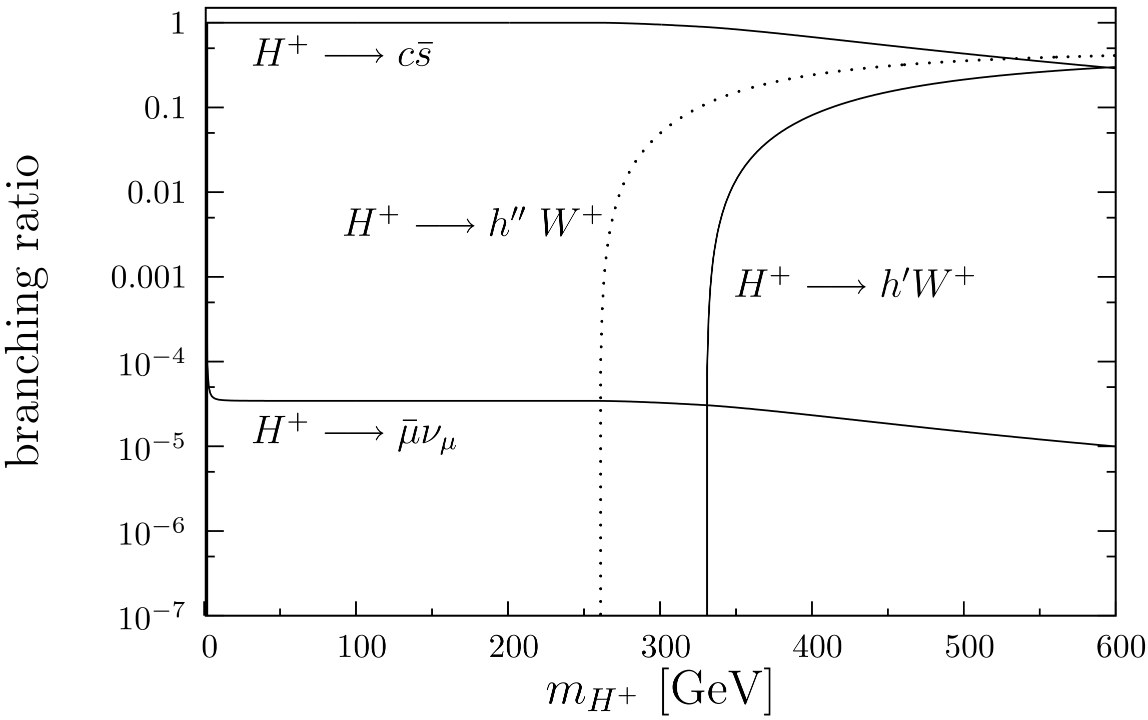

Figure 9. Branching fractions for the H^+ Higgs-boson decay channels as function of m_{H^+}. It is supposed that $m_{h'} = 250\,\text{GeV}$ and $m_{h''} = 180\,\text{GeV}$.

H_1	q	$\bar{q}'$	a	b	$\lvert a\rvert^2 + \lvert b\rvert^2$
ρ'	t	$\bar{t}$	m_t	0	m_t^2
	b	$\bar{b}$	m_b	0	m_b^2
h'	c	$\bar{c}$	$-m_t$	0	m_t^2
	s	$\bar{s}$	$-m_b$	0	m_b^2
h''	c	$\bar{c}$	0	im_t	m_t^2
	s	$\bar{s}$	0	$-im_b$	m_b^2
H^+	c	$\bar{s}$	$\frac{1}{\sqrt{2}}(m_t - m_b)$	$\frac{1}{\sqrt{2}}(m_t + m_b)$	$m_t^2 + m_b^2$
H^-	s	$\bar{c}$	$\frac{1}{\sqrt{2}}(m_t - m_b)$	$-\frac{1}{\sqrt{2}}(m_t + m_b)$	$m_t^2 + m_b^2$

Table 5. The quark-antiquark fusion processes contributing to the Higgs-boson production (4.1) in the MCPM and the corresponding coupling constants in figure 11.

which can occur in the MCPM are listed in table 5 together with the coupling constants a and b in the diagram shown for the generic process in figure 11,

$$q(p_1') + \bar{q}'(p_2') \to H_1(k)\ . \tag{4.2}$$

For the ρ' we have a large coupling to the t quark. But even at LHC energies there are not many t and $\bar{t}$ quarks in the proton. Thus ρ' production via quark-antiquark fusion is unimportant in the MCPM. This conclusion is exactly as in the SM for ρ'_{SM}; see for instance [20].

For the h' and h'' we have a very large coupling proportional to m_t for c quarks. For the charged Higgs bosons H^+ and H^- there is a large coupling in the fusion processes with

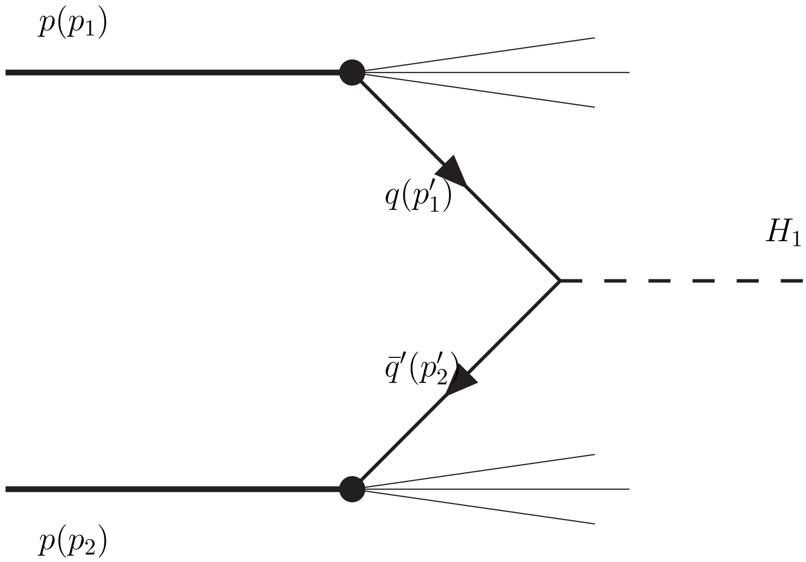

Figure 10. The generic diagram for the production of a Higgs particle H_1 via quark-antiquark fusion, $q\bar{q}' \to H_1$, in proton-proton collisions.

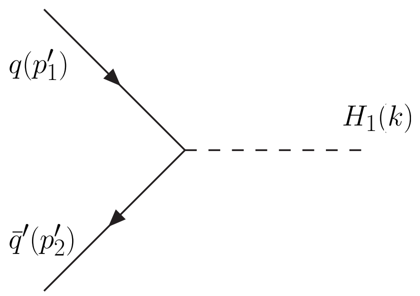

Figure 11. The generic diagram for the fusion process $q\bar{q}' \to H_1$ and the corresponding analytic expression for the vertex.

$c\bar{s}$ and $s\bar{c}$ quarks, respectively. There are plenty of c and s quarks in the proton at LHC energies. Thus, these processes contribute significantly to Higgs-boson production. The total cross section for the production of a Higgs boson H_1 via $q\bar{q}'$ fusion is easily evaluated from the diagrams of figures 10 and 11. We get with $s = (p_1 + p_2)^2$, the c.m. energy squared of the process (4.1), the following:

$$\sigma(p(p_1) + p(p_2) \to H_1(k) + X)|_{q\bar{q}'-\text{fusion}} = \frac{\pi}{3v_0^2 s}(|a|^2 + |b|^2)F_{q\bar{q}'}\left(\frac{m_{H_1}^2}{s}\right). \tag{4.3}$$

Here we define

$$F_{q\bar{q}'}\left(\frac{m_{H_1}^2}{s}\right) = \int_0^1 dx_1 N_q^p(x_1) \int_0^1 dx_2 N_{\bar{q}'}^p(x_2)\delta\left(x_1 x_2 - \frac{m_{H_1}^2}{s}\right) \tag{4.4}$$

where $N_q^p(x)$ and $N_{\bar{q}'}^p(x)$ are the quark and antiquark distribution functions of the proton, respectively, at LHC energies. From (4.3) and table 5 we get for the Drell-Yan type contributions to (4.1)

$$\sigma(p(p_1)+p(p_2)\to h'+X)\big|_{\rm DY} = \frac{\pi}{3v_0^2 s}\left[m_t^2 F_{c\bar{c}}\left(\frac{m_{h'}^2}{s}\right)+m_b^2 F_{s\bar{s}}\left(\frac{m_{h'}^2}{s}\right)\right], \tag{4.5}$$

$$\sigma(p(p_1)+p(p_2)\to h''+X)\big|_{\rm DY} = \frac{\pi}{3v_0^2 s}\left[m_t^2 F_{c\bar{c}}\left(\frac{m_{h''}^2}{s}\right)+m_b^2 F_{s\bar{s}}\left(\frac{m_{h''}^2}{s}\right)\right], \tag{4.6}$$

$$\sigma(p(p_1)+p(p_2)\to H^+ +X)\big|_{\rm DY} = \frac{\pi}{3v_0^2 s}(m_t^2+m_b^2)F_{c\bar{s}}\left(\frac{m_{H^+}^2}{s}\right), \tag{4.7}$$

$$\sigma(p(p_1)+p(p_2)\to H^- +X)\big|_{\rm DY} = \frac{\pi}{3v_0^2 s}(m_t^2+m_b^2)F_{s\bar{c}}\left(\frac{m_{H^-}^2}{s}\right). \tag{4.8}$$

The cross sections (4.5)–(4.8) are shown in figure 12 for $\sqrt{s} = 14$ TeV, corresponding to the energy available at the LHC, as function of the Higgs-boson masses. We also show in figure 12 the results for Higgs-boson production in proton-antiproton collisions for $\sqrt{s} =$ 1.96 TeV corresponding to the energy available at the Tevatron. Of course, for $p\bar{p}$ collisions the factor $F_{q\bar{q}'}$ in (4.3) and (4.4) has to be replaced by an integral over proton and antiproton distribution functions

$$F_{q\bar{q}'}\left(\frac{m_{H_1}^2}{s}\right) = \frac{1}{2}\int_0^1 dx_1 \int_0^1 dx_2 \Big(N_q^p(x_1)N_{\bar{q}'}^{\bar{p}}(x_2)+N_q^{\bar{p}}(x_1)N_{\bar{q}'}^{p}(x_2)\Big)\delta\left(x_1x_2-\frac{m_{H_1}^2}{s}\right). \tag{4.9}$$

We emphasize that all results of this subsection are obtained in the strict symmetry limit of the MCPM.

4.2 Higgs-boson production by gluon-gluon fusion

Here we study the production of the neutral Higgs particles ρ', h' and h'' via gluon-gluon fusion. The corresponding generic diagram is shown in figure 13. In leading order the gluons couple to the Higgs particle via a quark loop. The diagram of figure 13 is easily evaluated and gives for the total cross section

$$\sigma(p(p_1)+p(p_2)\to H_1+X)\big|_{GG-\rm fusion} = \frac{\pi^2\Gamma(H_1\to GG)}{8\;s\;m_{H_1}}F_{\rm GG}\left(\frac{m_{H_1}^2}{s}\right), \tag{4.10}$$

where $H_1 = \rho', h'$, and h''. The function $F_{\rm GG}$ is defined as

$$F_{\rm GG}\left(\frac{m_{H_1}^2}{s}\right) = \int_0^1 dx_1 N_G^p(x_1)\int_0^1 dx_2 N_G^p(x_2)\delta\left(x_1x_2-\frac{m_{H_1}^2}{s}\right) \tag{4.11}$$

with $N_G^p(x)$ the gluon distribution function of the proton at LHC energies. Furthermore, $\Gamma(H_1\to GG)$ is the partial decay width for H_1 decaying into two gluons as discussed in section 3.4.

Setting $H_1 = \rho'$ in (4.10) and using $\Gamma(\rho'\to GG)$ from (3.22) we get the cross section for ρ' production via gluon-gluon fusion in the MCPM. The result as shown in figure 14 is valid in the strict symmetry limit of the MCPM and coincides with that from the SM

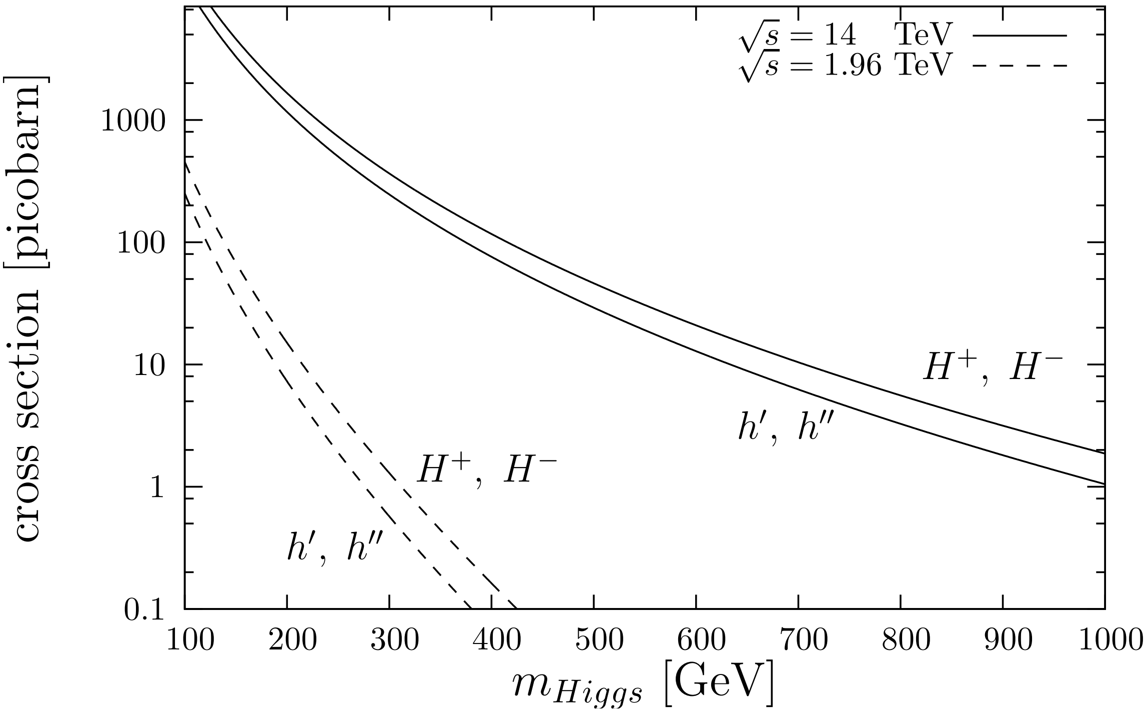

Figure 12. The cross sections for Higgs-boson production via quark-antiquark fusion for proton-proton collisions at LHC energies (full lines) and for proton-antiproton collisions at Tevatron energies (dashed lines), respectively, as functions of the Higgs-boson masses.

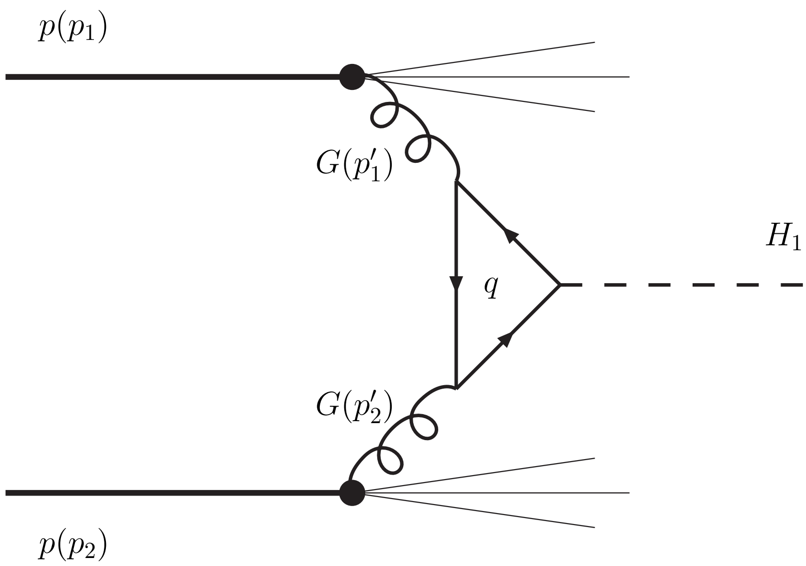

Figure 13. Diagram for the production of a Higgs particle H_1 by gluon-gluon fusion in proton-proton collisions.

for $\rho'_{\rm SM}$; see for instance [22]. Setting successively $H_1 = h'$ and $H_1 = h''$ in (4.10) we obtain with (3.23) and (3.24) our estimates, in the sense discussed at the end of section 3, for the corresponding production cross sections as shown in figure 14. Again, we give

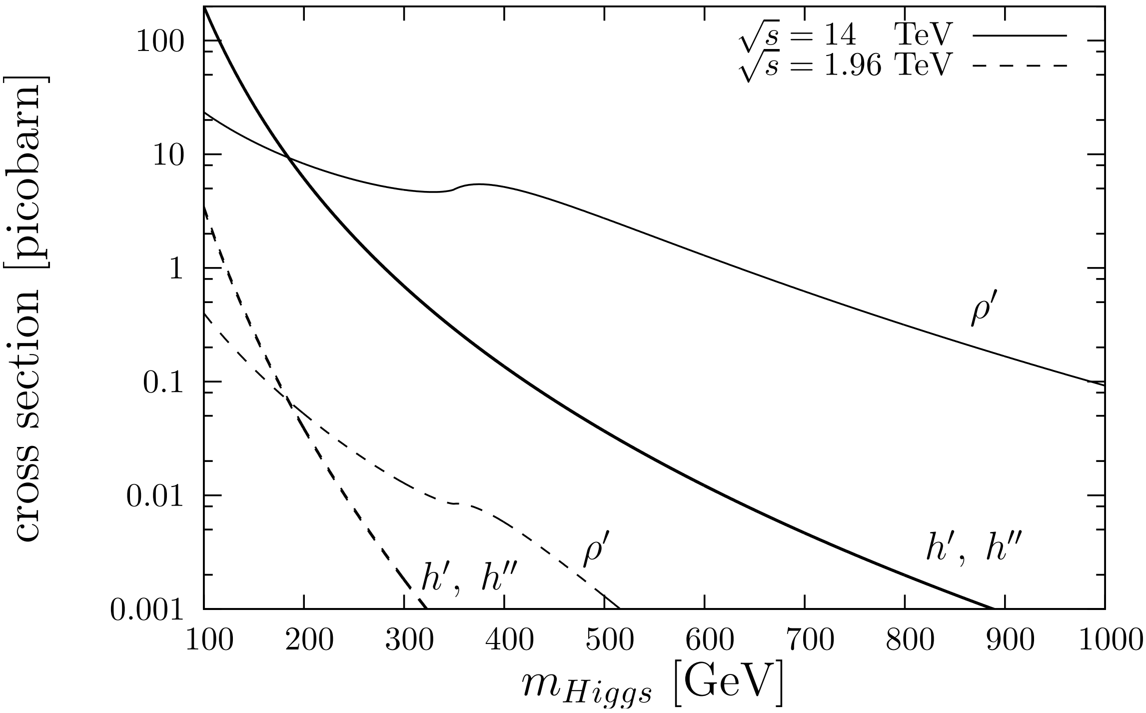

Figure 14. The cross sections for the production of ρ', h' and h'' via gluon-gluon fusion as functions of the Higgs-boson masses in proton-proton collisions at a c.m. energy of $\sqrt{s} = 14$ TeV (full lines) and in proton-antiproton collisions at $\sqrt{s} = 1.96$ TeV (dashed lines), respectively.

in figure 14 also the cross sections for Higgs-boson production via gluon-gluon fusion in proton-antiproton collisions at $\sqrt{s} = 1.96\,\text{TeV}$.

5 Discussion and conclusions

In this article we have given phenomenological predictions for proton-proton collisions at LHC energies in the framework of a two-Higgs-doublet model satisfying the principle of maximal CP invariance as introduced in [19]. In this maximally-CP-symmetric model (MCPM) there are three neutral Higgs particles, ρ', h' and h'', and one charged Higgs-boson pair $H^{\pm}$. We have investigated the decays of these particles. The Higgs particle ρ' behaves practically as the Higgs particle $\rho'_{\rm SM}$ in the SM. Only the 2γ widths of ρ' and $\rho'_{\rm SM}$ may differ substantially for $m_{\rho'} \gtrsim 300\,\text{GeV}$. The particles h', h'' and $H^{\pm}$, on the other hand, are predicted to have quite interesting properties. They couple to the fermions of the second family with coupling constants given by the masses of the third family. As a consequence the main decays of these Higgs particles are the fermionic ones of table 3 if the Higgs masses are below about 400 GeV. For larger Higgs-boson masses, the decay into a lighter Higgs boson associated with a gauge boson may become dominant, as shown in examples by the branching ratios in figures 8 and 9.

We have studied the production of the Higgs bosons h' and h'' in proton-proton and proton-antiproton collisions via quark-antiquark and gluon-gluon fusion. We have found that the much higher gluon densities compared to the quark densities in the proton do not compensate the loop suppression of the leading order gluon-gluon fusion process. Thus we find the Drell-Yan process with the annihilation of $c\bar{c}$ quarks dominating the production cross sections for h' and h''. The Drell-Yan process also leads to a similar production cross section for H^+ and H^- via the annihilation of $c\bar{s}$ and $s\bar{c}$ quarks, respectively. In this way we get for the Higgs bosons h', h'' and $H^\pm$, if their masses are below 400 GeV, quite high production cross sections exceeding 100 pb at LHC energies. This is shown in figure 12. With an integrated luminosity of 100 fb^{-1} this translates into the production of more than 10^8 Higgs bosons of the types h', h'' and $H^\pm$ if their masses are around 200 GeV. For Higgs-boson masses of 400 GeV the number of produced particles h', h'' and $H^\pm$ is predicted to be of order 10^7. These produced Higgs bosons will mainly decay into c- and s-quarks giving two jets. But, of course, there is a very large background from ordinary QCD two-jet events. Perhaps it will be possible to detect the Higgs-boson production events over the QCD background using c-quark tagging. Clearly, this presents an experimental challenge. A further possibility is to use the information from the angular distribution of the two jets. For the decays of the scalar particles h', h'' and $H^\pm$ the two-jet angular distributions must be isotropic in the rest frame of the decaying particle. Contrary to this, the QCD two-jet events are peaked in the beam directions. Clearly, only a detailed Monte Carlo study including an investigation of the QCD background and the detector resolution can tell if the particles h', h'' and $H^\pm$ are observable in their two-jet decays with the LHC detectors.

A promising signal for detecting the Higgs bosons h', h'' and $H^\pm$ of the MCPM is provided by their leptonic decays

$$\begin{aligned} h' &\to \mu^+\mu^- \,, \\ h'' &\to \mu^+\mu^- \,, \\ H^+ &\to \mu^+\nu_\mu \,, \\ H^- &\to \mu^-\bar{\nu}_\mu \,. \end{aligned} \tag{5.1}$$

In (3.25) we have estimated the branching fractions for these decays to be about 3×10^{-5} for Higgs-boson masses below 400 GeV. With an integrated luminosity of 100 fb^{-1} and the number of produced Higgs bosons given above we predict then around 3000 leptonic events for each of the channels in (5.1) if the Higgs-boson masses are around 200 GeV. For Higgs-boson masses of 400 GeV we still have 300 leptonic events for each of the decays in (5.1). We emphasize that a distinct feature of the MCPM is that decays involving the leptons τ and ν_τ as well as e and ν_e should be highly suppressed compared to the muonic channels (5.1). We may note that the $\mu^+\mu^-$ channel will be prominent at the LHC for the search for new effects including for instance heavy Z' bosons or Kaluza-Klein particles, see for instance [23, 24]. Thus, the suppression of the τ and e channels for the Higgs bosons of the MCPM may be an important way for distinguishing the MCPM from other possibilities for physics beyond the SM.

To conclude, we have in this article presented concrete predictions for the production and decay of the Higgs bosons of the MCPM. We found the Drell-Yan type process to be the dominant production mechanism. But, of course, there are also other mechanisms,

JHEP05(2009)028

which we hope to investigate in future work, for instance, Higgs-strahlung in quark-quark collisions. Thus, the predicted numbers of produced Higgs bosons given above for the LHC are in fact lower limits. We are looking forward to the start up of the experimentation at the LHC, where it should be possible to check our predictions.

Acknowledgments

It is a pleasure for the authors to thank P. Braun-Munzinger, C. Ewerz, G. Ingelman, A. v.Manteuffel and H.C. Schultz-Coulon for useful discussions and suggestions. Thanks are due to A. v.Manteuffel and D. Stöckinger for reading of the manuscript.

A The Lagrangian after EWSB

The task is to express the Lagrangian $\mathscr{L}$ of the MCPM in terms of physical fields in the unitary gauge. This Lagrangian is given by

$$\mathscr{L} = \mathscr{L}_\varphi + \mathscr{L}_{\text{Yuk}} + \mathscr{L}_{\text{FB}} \tag{A.1}$$

where $\mathscr{L}_{\text{FB}}$ is the standard gauge kinetic term for the fermions and gauge bosons; see for instance [25]. The Higgs-boson Lagrangian is denoted by $\mathscr{L}_\varphi$, the Yukawa term, giving the coupling of the fermions to the Higgs fields, by $\mathscr{L}_{\text{Yuk}}$. In [18, 19] the form for $\mathscr{L}_\varphi$ and $\mathscr{L}_{\text{Yuk}}$ was derived from the requirement of maximal CP invariance, absence of flavor-changing neutral currents and absence of mass-degenerate massive fermions. For $\mathscr{L}_\varphi$ the result is

$$\mathscr{L}_\varphi = \sum_{i=1,2} \left(D_\mu \varphi_i\right)^\dagger \left(D^\mu \varphi_i\right) - V(\varphi_1, \varphi_2)\;, \tag{A.2}$$

where D_μ are the covariant derivatives and V is given in (2.11). The Yukawa term, $\mathscr{L}_{\text{Yuk}}$, is given in (2.13).

Using the unitary gauge we insert for the Higgs-boson fields φ_1 and φ_2 the expressions (2.15) and (2.16), respectively. In the following we use as independent parameters of the Lagrangian the fine structure constant α, respectively $e = \sqrt{4\pi\alpha}$, the Fermi constant G_F, the mass m_Z of the Z-boson, the Higgs-boson masses $m^2_{\rho'}$, $m^2_{h'}$, $m^2_{h''}$, $m^2_{H^\pm}$, see (2.17)–(2.20), and the fermion masses m_τ, m_t, m_b; see (2.22). With this, the following parameters are dependent ones: $s_W \equiv \sin\theta_W$, $c_W \equiv \cos\theta_W$, where θ_W is the weak mixing angle, the mass m_W of the W boson, and the VEV v_0. The corresponding tree-level expressions for them in terms of the independent parameters are

$$\begin{aligned} s^2_W &= \frac{1}{2}\left[1 - \left(1 - \frac{e^2}{\sqrt{2} G_F m^2_Z}\right)^{1/2}\right], \\ m^2_W &= \frac{m^2_Z}{2}\left[1 + \left(1 - \frac{e^2}{\sqrt{2} G_F m^2_Z}\right)^{1/2}\right], \\ v_0 &= 2^{-1/4} G_F^{-1/2}\,. \end{aligned} \tag{A.3}$$

Keeping this in mind we find for K_0–K_3 of (2.4), inserting (2.15) and (2.16),

$$\begin{aligned} K_0 &= \frac{1}{2}(v_0+\rho')^2 + \frac{1}{2}(h'^2+h''^2) + H^+H^- \,, \\ K_1 &= (v_0+\rho')h' \,, \\ K_2 &= (v_0+\rho')h'' \,, \\ K_3 &= \frac{1}{2}(v_0+\rho')^2 - \frac{1}{2}(h'^2+h''^2) - H^+H^- \,. \end{aligned} \tag{A.4}$$

We get from (A.1) the following explicit form of $\mathscr{L}$. The expression for the fermion-boson term $\mathscr{L}_{\rm FB}$ is standard and can be found for instance in [25]. For $\mathscr{L}_\varphi + \mathscr{L}_{\rm Yuk}$ we get

$$\begin{aligned} \mathscr{L}_\varphi + \mathscr{L}_{\rm Yuk} = & \frac{1}{8}m_{\rho'}^2 v_0^2 + \frac{1}{2}(\partial_\mu\rho')(\partial^\mu\rho') + m_W^2 W_\mu^- W^{+\,\mu}\left(1+\frac{\rho'}{v_0}\right)^2 \\ & + \frac{1}{2}m_Z^2 Z_\mu Z^\mu \left(1+\frac{\rho'}{v_0}\right)^2 + (\partial_\mu H^+)(\partial^\mu H^-) \\ & + \frac{1}{2}(\partial_\mu h')(\partial^\mu h') + \frac{1}{2}(\partial_\mu h'')(\partial^\mu h'') \\ & - \frac{1}{2}m_{\rho'}^2\left(\rho'^2 + \frac{1}{v_0}\rho'^3 + \frac{1}{4v_0^2}\rho'^4\right) \\ & - \frac{1}{2}m_{h'}^2 h'^2 - \frac{1}{2}(m_{\rho'}^2 + 2m_{h'}^2)h'^2\left[\frac{1}{v_0}\rho' + \frac{1}{2v_0^2}\rho'^2\right] \\ & - \frac{1}{2}m_{h''}^2 h''^2 - \frac{1}{2}(m_{\rho'}^2 + 2m_{h''}^2)h''^2\left[\frac{1}{v_0}\rho' + \frac{1}{2v_0^2}\rho'^2\right] \\ & - m_{H^\pm}^2 H^+H^- - (m_{\rho'}^2 + 2m_{H^\pm}^2)H^+H^-\left[\frac{1}{v_0}\rho' + \frac{1}{2v_0^2}\rho'^2\right] \\ & - \frac{m_{\rho'}^2}{2v_0^2}\left[\frac{1}{4}(h'^4 + h''^4 + 2h'^2h''^2) + (h'^2+h''^2)H^+H^- + (H^+)^2(H^-)^2\right] \\ & + ie\left(\frac{c_W^2 - s_W^2}{2s_W c_W}Z^\mu + A^\mu\right)(H^+\partial_\mu H^- - H^-\partial_\mu H^+) \\ & + \frac{e}{2s_W c_W}Z^\mu(h''\partial_\mu h' - h'\partial_\mu h'') \\ & + \frac{ie}{2s_W}W^{+\,\mu}(h'\partial_\mu H^- - H^-\partial_\mu h') \\ & - \frac{ie}{2s_W}W^{-\,\mu}(h'\partial_\mu H^+ - H^+\partial_\mu h') \\ & - \frac{e}{2s_W}W^{+\,\mu}(h''\partial_\mu H^- - H^-\partial_\mu h'') \\ & - \frac{e}{2s_W}W^{-\,\mu}(h''\partial_\mu H^+ - H^+\partial_\mu h'') \\ & + e^2\left[\left(\frac{c_W^2 - s_W^2}{2s_W c_W}\right)^2 Z_\mu Z^\mu H^+H^- + \frac{c_W^2 - s_W^2}{s_W c_W}Z_\mu A^\mu H^+H^- + A_\mu A^\mu H^+H^-\right] \\ & + \frac{e^2}{8s_W^2 c_W^2}Z_\mu Z^\mu(h'^2+h''^2) \\ & + \frac{e^2}{2s_W^2}W_\mu^+ W^{-\,\mu}\left(\frac{1}{2}h'^2 + \frac{1}{2}h''^2 + H^+H^-\right) \end{aligned}$$

JHEP05(2009)028

$$
\begin{aligned}
&+\frac{e^2}{2s_W}\Big(-\frac{s_W}{c_W}Z_\mu + A_\mu\Big)W^{+\,\mu}H^- h' \\
&+\frac{e^2}{2s_W}\Big(-\frac{s_W}{c_W}Z_\mu + A_\mu\Big)W^{-\,\mu}H^+ h' \\
&+\frac{ie^2}{2s_W}\Big(-\frac{s_W}{c_W}Z_\mu + A_\mu\Big)W^{+\,\mu}H^- h'' \\
&-\frac{ie^2}{2s_W}\Big(-\frac{s_W}{c_W}Z_\mu + A_\mu\Big)W^{-\,\mu}H^+ h'' \\
&-m_\tau\bar{\tau}\tau\Big(1+\frac{1}{v_0}\rho'\Big) - m_t\bar{t}t\Big(1+\frac{1}{v_0}\rho'\Big) - m_b\bar{b}b\Big(1+\frac{1}{v_0}\rho'\Big) \\
&+\frac{m_\tau}{v_0}\bar{\mu}\mu h' + \frac{m_t}{v_0}\bar{c}ch' + \frac{m_b}{v_0}\bar{s}sh' \\
&+\frac{im_\tau}{v_0}\bar{\mu}\gamma_5\mu h'' - \frac{im_t}{v_0}\bar{c}\gamma_5 ch'' + \frac{im_b}{v_0}\bar{s}\gamma_5 sh'' \\
&+\frac{m_\tau}{\sqrt{2}v_0}\left[\bar{\nu}_\mu(1+\gamma_5)\mu H^+ + \bar{\mu}(1-\gamma_5)\nu_\mu H^-\right] \\
&-\frac{1}{\sqrt{2}v_0}\Big\{\bar{c}\left[m_t(1-\gamma_5) - m_b(1+\gamma_5)\right] sH^+ \\
&\qquad +\bar{s}\left[m_t(1+\gamma_5) - m_b(1-\gamma_5)\right] cH^-\Big\}.
\end{aligned}
\tag{A.5}
$$

From (A.5) it is easy to read off the Feynman rules in the unitary gauge. We list here only the Higgs-boson-fermion vertices and the vertices for two Higgs bosons and one gauge boson. The arrow on the W and H lines indicates the flow of negative charge. In case a momentum occurs in the Feynman rules, the momentum direction is indicated by an extra arrow.

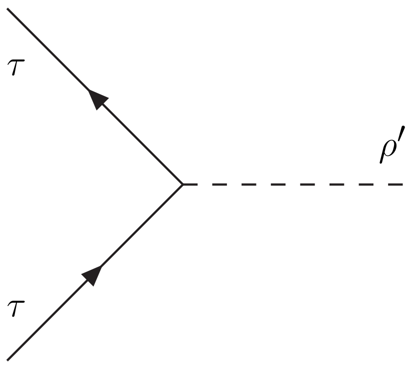

$-i\frac{m_\tau}{v_0}$

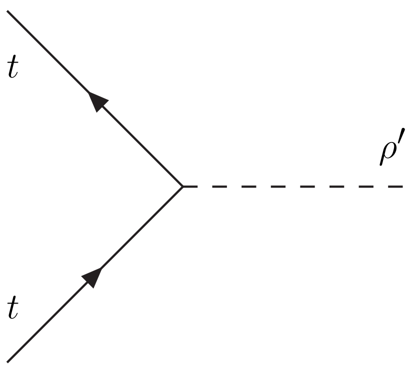

$-i\frac{m_t}{v_0}$

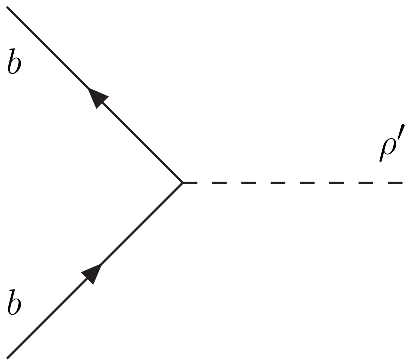

$-i\frac{m_b}{v_0}$

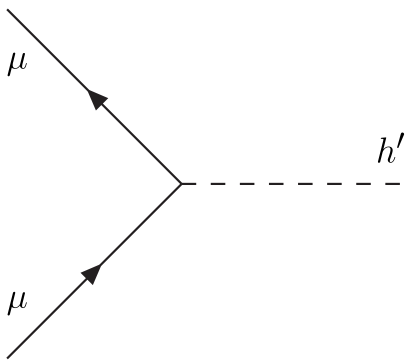

$i\frac{m_\tau}{v_0}$

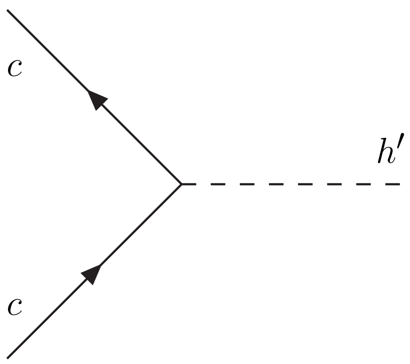

$i\frac{m_t}{v_0}$

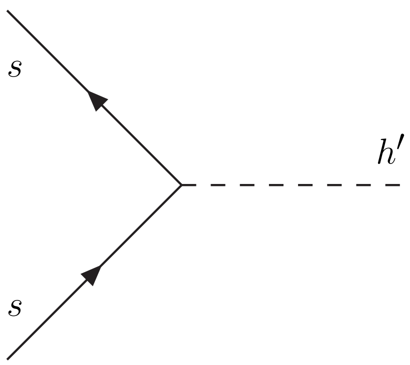

$i\frac{m_b}{v_0}$

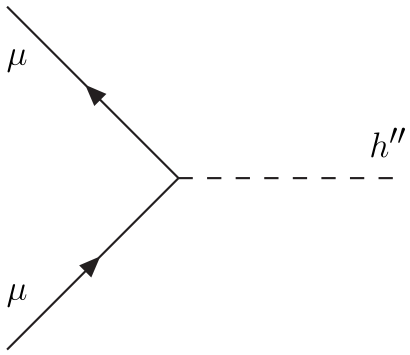

$-\frac{m_\tau}{v_0}\gamma_5$

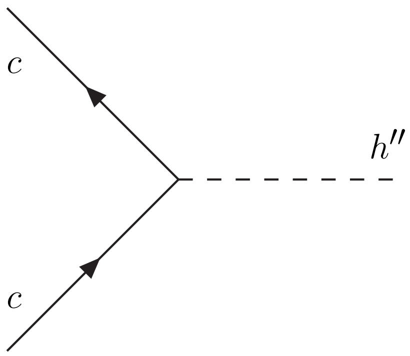

$\frac{m_t}{v_0}\gamma_5$

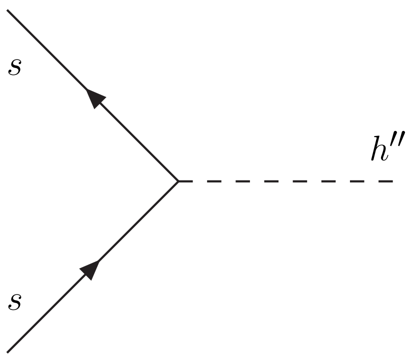

$-\frac{m_b}{v_0}\gamma_5$

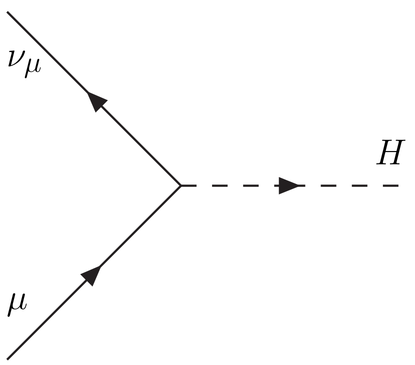

$i\frac{m_\tau}{\sqrt{2}v_0}(1+\gamma_5)$

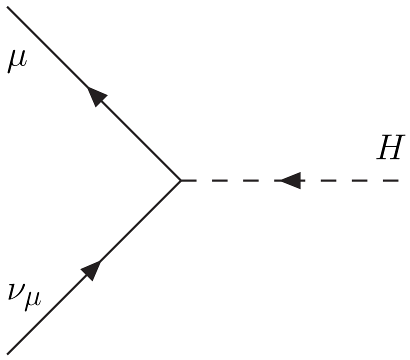

$$i\frac{m_\tau}{\sqrt{2}v_0}(1-\gamma_5)$$

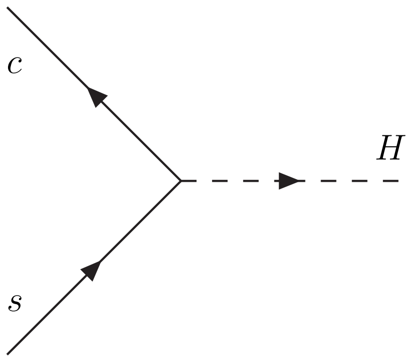

$$-i\frac{1}{\sqrt{2}v_0}\left[m_t(1-\gamma_5)-m_b(1+\gamma_5)\right]$$

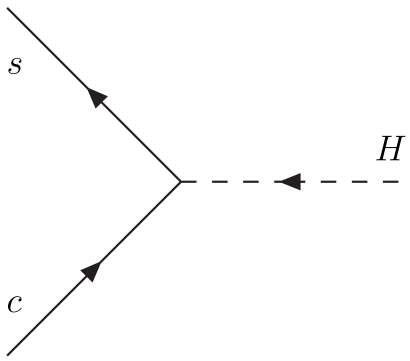

$$-i\frac{1}{\sqrt{2}v_0}\left[m_t(1+\gamma_5)-m_b(1-\gamma_5)\right]$$

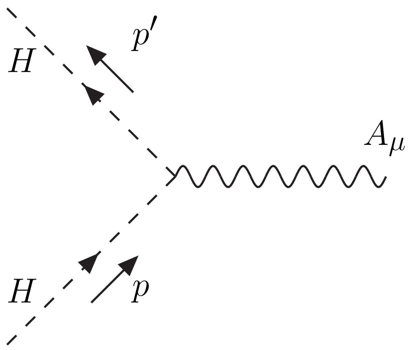

$$ie(p+p')_\mu$$

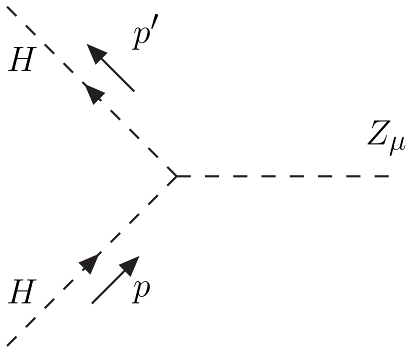

$$ie\frac{c_W^2 - s_W^2}{2s_W c_W}(p+p')_\mu$$

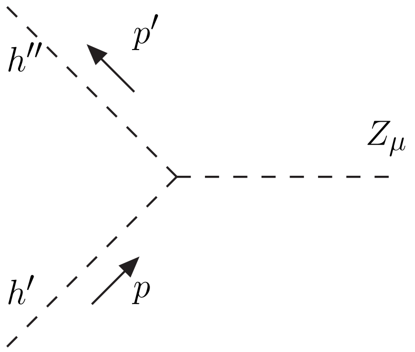

$$\frac{e}{2s_W c_W}(p+p')_\mu$$

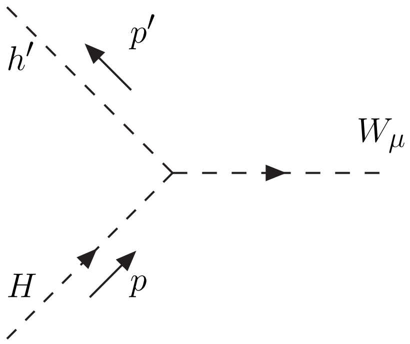

$$i\frac{e}{2s_W}(p+p')_\mu$$

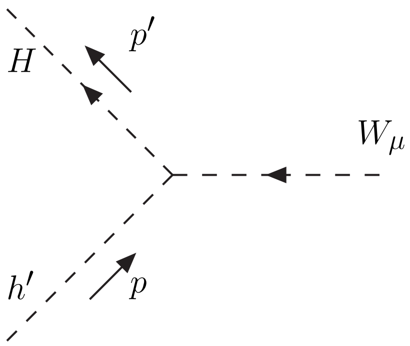

$$i\frac{e}{2s_W}(p+p')_\mu$$

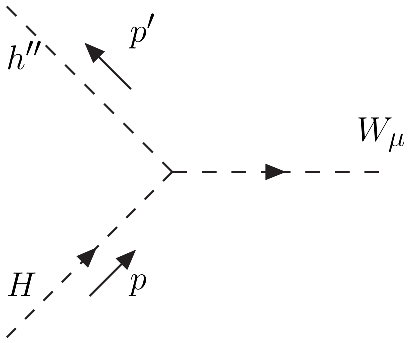

$$-\frac{e}{2s_W}(p+p')_\mu$$

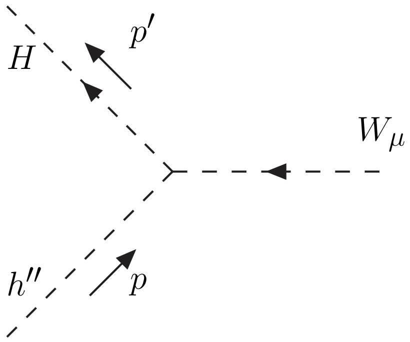

$$\frac{e}{2s_W}(p+p')_\mu$$

References

[1] Particle Data Group collaboration, C. Amsler et al., *Review of particle physics*, *Phys. Lett.* **B 667** (2008) 1 [SPIRES].

[2] J.R. Ellis, *Beyond the standard model at the LHC and beyond*, *AIP Conf. Proc.* **957** (2007) 38 [arXiv:0710.0777] [SPIRES].

[3] M. Kobayashi and T. Maskawa, *CP violation in the renormalizable theory of weak interaction*, *Prog. Theor. Phys.* **49** (1973) 652 [SPIRES].

[4] J.F. Gunion, H.E. Haber, G.L. Kane and S. Dawson, *The Higgs hunter's guide*, Addison-Wesley publishing company, (1990).

[5] G. Cvetič, *CP violation in bosonic sector of SM with two Higgs doublets*, *Phys. Rev.* **D 48** (1993) 5280 [hep-ph/9309202] [SPIRES].

[6] I.F. Ginzburg and M. Krawczyk, *Symmetries of two Higgs doublet model and CP-violation*, *Phys. Rev.* **D 72** (2005) 115013 [hep-ph/0408011] [SPIRES].

[7] J.F. Gunion and H.E. Haber, *Conditions for CP-violation in the general two-Higgs-doublet model*, *Phys. Rev.* **D 72** (2005) 095002 [hep-ph/0506227] [SPIRES].

[8] R. Barbieri and L.J. Hall, *Improved naturalness and the two Higgs doublet model*, hep-ph/0510243 [SPIRES].

[9] G.C. Branco, M.N. Rebelo and J.I. Silva-Marcos, *CP-odd invariants in models with several Higgs doublets*, *Phys. Lett.* **B 614** (2005) 187 [hep-ph/0502118] [SPIRES].

[10] C.C. Nishi, *CP violation conditions in N-Higgs-doublet potentials*, *Phys. Rev.* **D 74** (2006) 036003 [*Erratum ibid.* **D 76** (2007) 119901] [hep-ph/0605153] [SPIRES].

[11] R. Barbieri, L.J. Hall and V.S. Rychkov, *Improved naturalness with a heavy Higgs: an alternative road to LHC physics*, *Phys. Rev.* **D 74** (2006) 015007 [hep-ph/0603188] [SPIRES].

[12] I.P. Ivanov, *Minkowski space structure of the Higgs potential in* 2*HDM*, *Phys. Rev.* **D 75** (2007) 035001 [*Erratum ibid.* **D 76** (2007) 039902] [hep-ph/0609018] [SPIRES].

[13] L. Fromme, S.J. Huber and M. Seniuch, *Baryogenesis in the two-Higgs doublet model*, *JHEP* **11** (2006) 038 [hep-ph/0605242] [SPIRES].

[14] I.P. Ivanov, *Minkowski space structure of the Higgs potential in* 2*HDM: II. Minima, symmetries and topology*, *Phys. Rev.* **D 77** (2008) 015017 [arXiv:0710.3490] [SPIRES].

[15] A. Barroso, P.M. Ferreira and R. Santos, *Neutral minima in two-Higgs doublet models*, *Phys. Lett.* **B 652** (2007) 181 [hep-ph/0702098] [SPIRES].

[16] J.M. Gerard and M. Herquet, *A twisted custodial symmetry in the two-Higgs-doublet model*, *Phys. Rev. Lett.* **98** (2007) 251802 [hep-ph/0703051] [SPIRES].

[17] M. Maniatis, A. von Manteuffel, O. Nachtmann and F. Nagel, *Stability and symmetry breaking in the general two-Higgs-doublet model*, *Eur. Phys. J.* **C 48** (2006) 805 [hep-ph/0605184] [SPIRES].

[18] M. Maniatis, A. von Manteuffel and O. Nachtmann, *CP violation in the general two-Higgs-doublet model: a geometric view*, *Eur. Phys. J.* **C 57** (2008) 719 [arXiv:0707.3344] [SPIRES].

[19] M. Maniatis, A. von Manteuffel and O. Nachtmann, *A new type of CP symmetry, family replication and fermion mass hierarchies*, *Eur. Phys. J.* **C 57** (2008) 739 [arXiv:0711.3760] [SPIRES].

[20] C. Buttar et al., *Les Houches physics at TeV colliders* 2005*, standard model and Higgs working group: summary report*, hep-ph/0604120 [SPIRES].

[21] C.S. Kim, C. Yu and K.Y. Lee, *Probing CP-violating two Higgs doublet model through interplay between LHC and ILC*, hep-ph/0602076 [SPIRES].

[22] A. Djouadi, *The anatomy of electro-weak symmetry breaking. I: the Higgs boson in the standard model*, *Phys. Rept.* **457** (2008) 1 [hep-ph/0503172] [SPIRES].

[23] CMS collaboration, G.L. Bayatian et al., *CMS physics technical design report, volume II: physics performance*, *J. Phys.* **G 34** (2007) 995 [SPIRES].

[24] ATLAS collaboration, *ATLAS detector and physics performance. Technical design report*, ATLAS-TDR-14 [CERN-LHCC-99-14] Vol. 2, (1999), available at http://atlas.web.cern.ch/Atlas/GROUPS/PHYSICS/TDR/access.html [SPIRES].

[25] O. Nachtmann, *Elementary particle physics: concepts and phenomena*, Springer, Berlin Germany (1990) [SPIRES].